Title
MEASUREMENTS OF QUANTUM NOISE IN RESISTIVELY SHUNTED JOSEPHSON JUNCTIONS

Authors
Koch, R.H.
Harlingen, D.J. Van
Clarke, J.

Publication Date
1981-09-01

LBL-13326
Preprint

Lawrence Berkeley Laboratory
UNIVERSITY OF CALIFORNIA

Materials & Molecular Research Division

Submitted to Physical Review B

MEASUREMENTS OF QUANTUM NOISE IN RESISTIVELY SHUNTED JOSEPHSON JUNCTIONS

Roger H. Koch, D.J. Van Harlingen, and John Clarke

September 1981

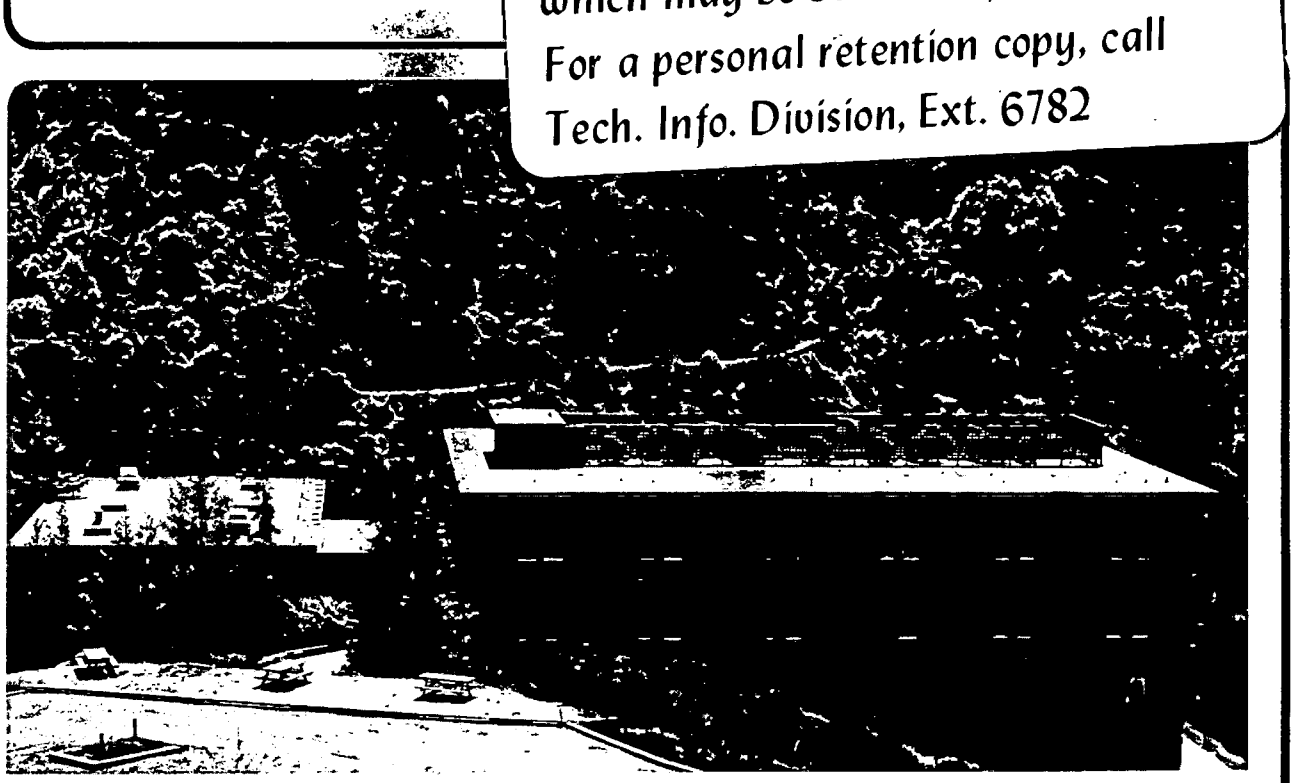

Prepared for the U.S. Department of Energy under Contract W-7405-ENG-48

DISCLAIMER

Submitted to The Physical Review B1
PACS 74.50.+r, 05.04.+j

LBL-13326

MEASUREMENTS OF QUANTUM NOISE IN RESISTIVELY SHUNTED JOSEPHSON JUNCTIONS

Roger H. Koch, D. J. Van Harlingen,* and John Clarke

Department of Physics, University of California
Berkeley, California 94720

and

Materials and Molecular Research Division
Lawrence Berkeley Laboratory, Berkeley, California 94720

SEPTEMBER 1981

ABSTRACT

Measurements have been made of the low frequency spectral density of the voltage noise, $S_v(0)$, in current-biased resistively shunted Josephson tunnel junctions under conditions in which the noise mixed down from frequencies near the Josephson frequency (ν_J) to the measurement frequency ($\ll \nu_J$) is in the regime $h\nu_J > k_BT$. In this limit, quantum corrections to the mixed-down noise are important. The values of $S_v(0)$ measured on junctions with current-voltage (I-V) characteristics close to the predictions of the Stewart-McCumber model were in excellent agreement with the prediction of Koch, Van Harlingen, and Clarke for $I > I_o$, $S_v(0)/R_D^2 = (4k_BT/R) + (2eV/R)(I_o/I)^2\coth(eV/k_BT)$, with no fitted parameters. Here, R and R_D are the shunt and dynamic resistances, and I_o is the critical current in the absence of noise. In particular, the mixed-down noise at voltages

This work was supported by the Director, Office of Energy Research, Office of Basic Energy Sciences, Materials Sciences Division of the U.S. Department of Energy under Contract No. W-7405-ENG-48.

above 300 μV did not change significantly when the temperature was lowered from 4.2K to 1.6K, and was in excellent agreement with the prediction $(2eV/R)(I_o/I)^2$ that is valid when $h\nu_J \gg k_BT$. This result demonstrates that the limiting noise arises from zero point fluctuations in the shunt resistor. The mixed-down noise for a wide range of bias voltages was used to compute the spectral density of the current noise in the shunt resistor, $S_I(\nu)$, at frequency ν. With no fitted parameters, the measured value of $S_I(\nu)$ at frequencies up to 500 GHz was in excellent agreement with the Callen-Welton prediction $(2h\nu/R)\coth(h\nu/2k_BT)$ at 1.6K and 4.2K. The presence of the zero point term, $2h\nu/R$, at frequencies $h\nu > k_BT$ was clearly demonstrated. The current-voltage characteristics of a junction with $\beta_L \equiv 2\pi LI_o/\Phi_o \sim 0.5$ and $\beta_C \equiv 2\pi I_o R^2 C/\Phi_o \ll 1$, where C is the junction capacitance and L_s is the shunt inductance, showed structure at voltages where the Josephson frequency was near a subharmonic of the L_sC resonant frequency. The additional non-linearity of the I-V characteristic caused mixing down of noise near higher harmonics of the Josephson frequency, thereby greatly enhancing the measured voltage noise. The measured spectral density of the noise was in good agreement with that of a computer simulation in which the values of L_s and C were fitted to match the measured I-V characteristic. These data also clearly demonstrated the quantum corrections to the mixed-down noise, and, in particular, the presence of the zero point term.

I. INTRODUCTION

The effects of thermal noise on a resistively shunted[1,2] Josephson[3] junction (RSJ) have been extensively studied. The theories assume that the noise originates as Nyquist noise in the shunt resistor R. The junction is modeled as a particle moving in a tilted periodic potential, and the effect of the noise current is to induce random fluctuations in the angle of tilt. These fluctuations have two effects. First, they enable the phase of the junction to slip by 2π when the bias current, I, is less than the noise-free critical current, I_o, thereby producing a voltage pulse across the junction. This effect produces noise rounding of the I-V characteristics at low voltages, V; the noise rounding has been calculated by Ambegoakar and Halperin[4] and Vystavkin et al.[5] for the case C = 0 (C is the capacitance of the junction). Subsequently, Kurkijärvi and Ambegoakar[6] and Voss[7] computed the case $C \neq 0$. Second, the fluctuations generate a voltage noise when the junction is current biased at a non-zero voltage. Likharev and Semenov[8] and Vystavkin et al.[5] showed that for the C = 0 case in the limit $h\nu_J \ll k_B T$ ($\nu_J = 2eV/h$ is the Josephson frequency) and for frequencies much less than ν_J, the spectral density of the voltage noise is given by

$$S_v(0) = \frac{4k_B T R_D^2}{R}\left[1 + \frac{1}{2}\left(\frac{I_o}{I}\right)^2\right] . \qquad (1.1)$$

Here, R_D is the dynamic resistance. This result was derived on the assumption that the noise is sufficiently small that one can neglect departures of the I-V characteristic from that of the ideal RSJ,[1,2]

$$V = R\left(I^2 - I_o^2\right)^{\frac{1}{2}}. \tag{1.2}$$

Thus, Eq. (1.1) is not valid in the noise-rounded region $I < I_o$. Voss[7] and Koch and Clarke[9] computed the noise for the case $C \neq 0$. Experimental results are in good agreement with calculations for both the noise rounding[10] and voltage noise.[11]

For a junction voltage-biased on a self-resonant step, Stephen[12] has calculated the contribution of pair current fluctuations to the linewidth of the Josephson radiation. This noise arises from photon number fluctuations (including zero point fluctuations) in the lossy cavity formed by the junction, and is not intrinsic to the tunneling of Cooper pairs in a non-resonant junction. Experimental results[13] are in good agreement with the predictions.

More recently, Koch et al.[14] considered the limit $h\nu_J \gtrsim k_B T$ in which quantum corrections to the noise generated in the shunt resistor become important. The equation of motion for the junction is

$$\frac{\hbar C}{2e}\ddot{\delta} + \frac{\hbar}{2eR}\dot{\delta} + I_o \sin\delta = I + I_N\ , \tag{1.3}$$

where δ is the phase difference across the junction, and the noise current, $I_n(t)$, has a spectral density[15]

$$S_I(\nu) = \frac{2h\nu}{R}\coth\left(\frac{h\nu}{2k_B T}\right)$$

$$= \frac{4h\nu}{R}\left[\frac{1}{\exp(h\nu/k_B T) - 1} + \frac{1}{2}\right]. \tag{1.4}$$

In the limit[1,2] $0 < \beta_c \equiv 2\pi I_o R^2 C/\Phi_o \ll 1$ ($\Phi_o \equiv h/2e$), the first term on the left-hand side of Eq. (1.3) can be neglected, and the equations can then be solved analytically using the techniques of Likharev and Semenov.[8] At frequencies much less than ν_J and in the limit $I/I_o > 1$ in which noise rounding can be neglected, the spectral density of the voltage noise, $S_v(0)$, is given by

$$\frac{S_v(0)}{R_D^2} = \frac{4k_BT}{R} + \frac{2eV}{R}\left(\frac{I_o}{I}\right)^2 \coth\left(\frac{eV}{k_BT}\right) . \tag{1.5}$$

The first term on the right-hand side is noise generated at the measurement frequency, while the second term is noise generated near the Josephson frequency that is mixed down to the measurement frequency by the nonlinearity of the junction. The contribution of noise generated near frequencies $2\nu_J$, $3\nu_J$ ... is negligible in the ideal RSJ model.

Equation (1.5) reduces to Eq. (1.1) in the limit $eV \ll k_BT$. In the limit $eV \gtrsim k_BT$, quantum corrections to the mixed-down noise become important, and the second term will become comparable to the first term on the right-hand side of Eq. (1.5) when $eV(I_o/I)^2 \gtrsim 2k_BT$. These requirements can be met provided $\kappa \gtrsim 1$, where

$$\kappa \equiv eI_oR/k_BT . \tag{1.6}$$

In the extreme quantum limit, $eV \gg k_BT$, Eq. (1.5) reduces to

$$\frac{S_v(0)}{R_D^2} = \frac{2eV}{R}\left(\frac{I_o}{I}\right)^2 , \tag{1.7}$$

and the observed noise is generated solely by zero point fluctuations in the shunt resistor. In our picture, the resistor can be modeled as a large collection of harmonic oscillators. In the ground state at $T = 0$, where there are no thermal fluctuations, the zero point energy still induces fluctuations in the tilted periodic potential, thus generating a randomness in the rate at which the phase, δ, propagates.

This model also predicts "quantum activation," that is, a noise rounding of the I-V characteristic of an overdamped junction ($\beta_c < 1$) even at $T = 0$ due to zero point fluctuations. Although we cannot yet make any quantitative statements, we suspect this description will fail when I becomes significantly smaller than I_o. In this limit, transitions out of the zero voltage state become very infrequent, and the model represented by Eq. (1.3) in which the particle is a point mass is likely to become invalid. Instead, one must treat the particle as a quantum mechanical wavepacket, which has some probability of penetrating the barrier by macroscopic quantum tunneling (MQT), as has been calculated by several authors.[16-19] Clearly, a quantitative theory that can deal with both zero point fluctuations and MQT for all values of the bias current and damping is very much needed.

In this paper we describe measurements of the voltage noise in current-biased overdamped junctions ($\beta_c < 1$) in the free-running mode $I > I_o$. In Sec. II we describe the experimental procedures, and in Sec. III we present the experimental results and compare them with the predictions of the theory. Section IV contains some concluding remarks.

II. EXPERIMENTAL PROCEDURES

A. Junction Fabrication

To observe quantum noise effects, we require junctions with $\kappa \gtrsim 1$. Writing $\kappa = (e/k_B T)(\beta_c \Phi_o j_1/2\pi c)^{\frac{1}{2}}$, where j_1 is the critical current density and c is the capacitance per unit area, we see that junctions with high critical current densities are necessary to observe these effects in the liquid He^4 temperature range. At 4.2K, with $\beta_c = 0.2$, $j_1 = 10^4$A cm^{-2} and c = 0.04pF μm^{-2} we find $\kappa \approx 1.1$. This is a convenient value of κ, since, as the temperature is lowered to near 1K, κ increases so that quantum effects become dominant.

Our PbIn-In_2O_3-Pb tunnel junctions, resistively shunted with CuAℓ films, were fabricated on glass substrates using the photolithographic lift-off techniques described by workers at IBM.[20] The configuration is shown in Fig. 1(a). We first deposited a 10 μm-wide Cu (0-3 wt.% Aℓ) film 40 to 100 nm thick, and then evaporated a 10 μm-wide, 250 nm-thick Pb (20 wt.% In) film at right angles to the CuAℓ strip. After another resist patterning, a SiO oxide layer, 100 nm thick, was deposited and two windows were opened by lifting off the SiO to expose the PbIn and CuAℓ films. After patterning the resist for the upper electrode, the exposed metal surfaces were cleaned by rf sputter-etching in Ar, the In_2O_3 oxide was grown thermally in a low pressure of oxygen, and the 400 nm-thick Pb counter-electrode was deposited and lifted off. A final protective layer of SiO was then evaporated. The diameter of the junction was about 2.5 μm, and the critical current ranged from 0.1 to 2 mA (0.2 to 4×10^4 A cm^{-2}) at 4.2K, depending on the oxidation parameters. The capacitance of the junction was estimated to be 0.5 pF (see Sec. III.D.). The resist-

ive shunt was about 5 μm long and ranged in resistance from 0.05 to 0.7 Ω, depending on the thickness and composition of the CuAℓ. The Pb counterelectrode formed a ground plane for the shunt, reducing its inductance, L_s, to about 0.2 pH. The critical currents of these junctions proved to be quite reproducible for a given set of oxidation conditions, and the junctions could be recycled between room and liquid helium temperatures at least several times without significant deterioration. We found that storing the junctions at room temperature for (say) 24 hours caused their critical currents to decrease (up to a factor of 2), while annealing them at 70°C for (say) 1 hour caused their critical currents to increase. Thus, if necessary, we could adjust the critical current somewhat, as we did with junction 3. Leads were attached to the junctions with pressed In pellets.

Junctions fabricated with these techniques omitting the resistive shunts displayed excellent tunneling characteristics with little excess current at voltages below the sum of the gaps.

B. Measurement Procedures

Before measuring the noise of a given junction, we plotted its I-V characteristic and dynamic resistance on a X-Y recorder, thus determining its critical current and the presence of any resonant structure. By applying an external magnetic field or by trapping the critical current to near zero we obtained the shunt resistance.

The noise measurement procedures now to be described were those that we used in the later measurements where most of the data were collected. Small modifications to the procedures used in the earlier work will be mentioned at the appropriate places in Sec. III. The circuit for measuring the noise across a junction is shown in Fig. 1(b). The bias current

was filtered by two low-pass filters each consisting of a cooled 1.5 kΩ resistor, R_F, and the cable capacitance, C_c. The junction was connected across two cooled LC-resonant circuits with inductors L_{t1}, L_{t2} and capacitors C_{t1}, C_{t2} (in fact, four-terminal connections were used). In a typical experiment, L_{t1} = 69 μH, L_{t2} = 35 μH, C_{t1} = 75 nF, and C_{t2} = 21.5 nF, giving resonant frequencies of 70 and 183 kHz. The leads across each tank circuit were connected in turn to a Brookdeal 5004 preamplifier to measure the noise across the junction at the appropriate frequency. In addition, by connecting together the leads across the tank circuits at the top of the cryostat we could measure the noise at a third, intermediate frequency, about 106 kHz for the values given above. After further amplification, the noise from the preamplifier was mixed down to frequencies below 500 Hz using a PAR 124. After low-pass filtering, the spectral density of the noise was measured using a PDP-11 computer. The junction, which was immersed directly in liquid He^4, was enclosed in a lead can, and the cryostat was surrounded by a mu-metal shield. The cryostat, bias supply, and preamplifier were enclosed in a shielded room.

To make the noise measurements, we first adjusted the bias current through the junction to obtain the required voltage, which was measured with a high-impedance voltmeter. We measured the voltage noise with the appropriate resonant circuit, using a typical averaging time of 10 min. The noise produced by the junction across the tank circuit was $Q^2 S_v(0) = \omega^2 L_t^2 [S_v(0)/R_D^2]$, so that the required quantity $S_v(0)/R_D^2$ was independent of Q. We note that the predicted value of $S_v(0)/R_D^2$ is virtually independent of β_c in the range $0 < \beta_c \lesssim 0.5$, while the value of $S_v(0)$ does increase significantly as β_c is increased in this range.[7,9] Thus, for β_c appreci-

ably greater than zero (junctions 2 and 3), it is much more reasonable to compare experimental and theoretical values of $S_v(0)/R_D^2$, rather than values of $S_v(0)$. However, a knowledge of the tank circuit impedance, Q^2R_D, was required to enable us to subtract the preamplifier current noise. We determined Q at each bias point by exciting the tank circuit inductively and measuring the half-power frequencies, using a function generator. From time to time during the noise measurements, the gain of the preamplifier-mixer-computer chain was calibrated by measuring the Nyquist noise across a room-temperature resistor R_c (5.1 kΩ) connected to the input of the preamplifier. We estimate the accuracy of the gain to be ± 2%. These measurements of the noise and of Q were repeated at each of the three frequencies for a series of voltages at each temperature and for a range of temperatures. Below 4.2K, the temperature of the helium bath was controlled by regulating the vapor pressure.

We now discuss the various measured corrections to the noise:
(i) The spectral densities of the voltage noise contributed by the preamplifier voltage noise (typically 6.1×10^{-19} V^2Hz^{-1} at 183 kHz) and current noise (typically 2.8×10^{-26} A^2Hz^{-1} at 183 kHz) were subtracted from the measured spectral density. The spectral density of the current noise was measured in a separate experiment by measuring the voltage noise across a cooled LC-resonant circuit containing a known resistor. The spectral density of the voltage noise was obtained during each set of measurements on a junction by shorting the input of the preamplifier. Because the current noise was checked less frequently than the voltage noise, we designed the tank circuits so that the contribution of the former was typically 25% of the latter. The total preamplifier noise was comparable with the junction noise at 4.2K, and as much as three times higher than the junction noise at 1.6K; the corresponding errors introduced by the correction varied

from ± 5% to ± 15% of the spectral density of the noise in the junction.

(ii) Losses in the tank circuit (for example, due to the presence of stray resistance) are a source of noise. The spectral density of this contribution was quite negligible (< 0.1%) for the 70- and 183-kHz tank circuits. However, the 106-kHz tank circuit contained two leads parts of which were at room temperature. Their noise contribution was measured with the junction in the zero resistance state, and was typically comparable with the spectral density of the voltage noise of the junction. The error in the correction at 106 kHz was ± 5%.

(iii) From the noise measurements at the three frequencies and at each bias voltage and temperature we determined that some junctions (2 and 4) generated a small excess noise with a spectral density very close to 1/f. The spectral density was proportional to $(\partial V/\partial I_o)^2$, suggesting that the noise arose from fluctuations in the critical current.[21] For example, for junction 2 the 1/f noise at 183 kHz was typically 5% of the spectral density of the voltage noise at the higher bias voltages, where $\partial V/\partial I_o$ became small. We subtracted the measured 1/f noise from the total junction noise at 183 kHz; even if the uncertainty in the noise was as high as 30%, the error introduced was no more than ± 3%.

(iv) The noise measurements were all performed at bias voltages well below the sum of the gaps of the two superconductors. The quasiparticle current contributes a noise with a current spectral density[13] $2eI_{qp}\coth(eV/2k_BT)$, where I_{qp} is the quasiparticle current. Thus, the ratio of the spectral density of the quasiparticle noise to the predicted spectral density of the mixed-down noise is of order $I_{qp}/(V/R)$, which we

estimate to be $\lesssim 10^{-2}$ at 4.2K over the voltage range of interest. At the lower temperatures, the quasiparticle current is substantially reduced, and its noise contribution is even smaller. Thus, we have neglected quasiparticle noise.

(v) The power dissipation in the shunt resistor caused its temperature to rise significantly above the bath temperature at the higher bias voltages in some junctions. For each junction we determined the heating effect as a function of temperature by reducing the critical current almost to zero and measuring the Nyquist noise of the shunt as a function of power dissipation. At low bias voltages the measured noise agreed with the Nyquist formula to within ± 3%. For most junctions the heating effect was important only at bias voltages $V \gg k_B T/e$, where the mixed-down term in Eq. (1.5) is nearly independent of the shunt temperature. Thus, it was sufficient to correct the data by subtracting the increase in the noise generated at the measurement frequency, $4k_B\Delta T/R$, from the measured value of $S_v(0)/R_D^2$, where ΔT is the temperature rise. In these cases, the heating correction was uncertain by ± 10% and was at most 30% of the total noise spectral density of the junction, thereby introducing a maximum error of ± 3% into the measurement. However, for junction 3, where the heating correction was particularly large, it was necessary to correct the mixed-down term as well by also subtracting $(4h\nu/R)\{[\exp(h\nu/k_BT^*) - 1]^{-1} - [\exp(h\nu/k_BT) - 1]^{-1}\}$ from the data, where $T^* = T + \Delta T$.

(vi) We took considerable care to shield the experiment from extraneous noise sources, and designed the measurement circuitry to avoid coupling significant 300K noise into the low-temperature circuitry. Measured values of the Nyquist noise in cooled resistors in the range 1.5 to 4.2K

were within ± 3% of the predicted value. Furthermore, measurements on junctions in the classical limit $eV \ll k_B T$ showed the correct temperature dependence and were in excellent agreement with theory (see Sec. III. A., B., and C.). Thus, we believe our measurements were not significantly influenced by extraneous noise sources.

III. EXPERIMENTAL RESULTS AND COMPARISON WITH THEORY

We report results on four different junctions that illustrate various aspects of the theory. The essential parameters of the junctions are listed in Table I.

A. Junction 1

As a test of our measurement system and of the effectiveness of the shielding we first investigated a junction in the limit $\kappa \ll 1$ in which the Likharev-Semenov[8] result, Eq. (1.1), is applicable. At 4.2K, the value of κ was 0.066. The parameters β_c and $\beta_L \equiv 2\pi L_s I_o/\Phi_o$ were 0.003 and 0.2, respectively, so that the I-V characteristic was very close to that for an ideal resistively shunted junction (see Sec. IV.D. for a discussion of the effects of the value of β_L). The 1/f and heating corrections were negligible throughout the range of measurement, so that the only corrections to the measured data were for preamplifier and tank circuit noise. (In this experiment, the measurements were at two frequencies only, 30 and 100 kHz.) In Fig. 2 we compare the measured noise with the predictions of Eq. (1.1). In plotting the theoretical points we used the predicted dynamic resistance[1,2]

$$R_D = R\left(1 - I_o^2/I^2\right)^{-\frac{1}{2}} \tag{3.1}$$

so that only the measured values of R, I_o, I, and T were used. Thus, we have neglected noise rounding,[4] and the predicted spectral density of the noise diverges as $I \to I_o$. Above the noise-rounded region, the agreement between theory and experiment is very good indeed. At very low voltages, the measured noise decreases as the current is lowered because the noise-rounded dynamic resistance decreases.

The good agreement between theory and experiment for $I > I_o$ indicates very strongly that the contribution of extraneous noise sources is negligible.

B. Junction 2

The parameters of this junction (Table I) were chosen to emphasize the quantum effects: Thus κ increased from 0.99 at 4.2K to 3.0 at 1.6K (the critical current increased slightly as the temperature was lowered). The values of β_c and β_L, about 0.38 and 0.31 at 4.2K, respectively, were small enough that the deviations from the ideal resistively shunted junction were relatively minor. Figure 3 shows I and dV/dI vs. V at 4.2K. There is a small drop in dV/dI at about 800 μV which we believe is associated with a resonance of the shunt inductance and the junction capacitance (see Sec. III.D.). There is also some very fine structure and a dip at 300 μV of unknown origin. We emphasize that in comparing the quantity $S_v(0)/R_D^2$ with the theory, small deviations in R_D from Eq. (3.1) will be suppressed provided the mixing coefficient $(I_o^2/2I^2)$ in Eq. (1.5) is not affected by the additional non-linearity. Another deviation from the simple model arose because the shunt resistance, R, which was measured with the critical current suppressed nearly to zero, varied between 0.65Ω and 0.75Ω as the voltage bias was increased from 0 to 1 mV. We

believe this variation was the result of a proximity effect between the shunt and the electrodes, or possibly of diffusion of Pb into the shunt. The measured value of R was used at each voltage bias when we compared theory and experiment.

In Fig. 4 we plot measured values of $S_v(0)/R_D^2$ vs. voltage (open circles) after the preamplifier noise has been subtracted. The solid circles are the noise after the 1/f noise subtraction and the heating correction have been made. At low voltages the correction is entirely due to 1/f noise, while at high voltages, the correction is largely due to heating. In the mid-voltage range, both corrections are small. The solid line through the solid circles is the prediction of Eq. (1.5) using the measured values of R, I_o, I, V, and T. The upper dashed line is the predicted noise in the absence of zero point fluctuations, that is

$$\frac{S_v'(0)}{R_D^2} = \frac{4k_BT}{R} + \frac{4eV}{R}\left(\frac{I_o}{I}\right)^2 \frac{1}{\exp(2eV/k_BT) - 1} . \qquad (3.2)$$

The triangles in Fig. 4 represent the measured mixed-down noise, which was computed by subtracting $4k_BT/R$ from the solid circles. The solid line through the triangles is the mixed-down noise prediced by Eq. (1.5), $(2eV/R)(I_o/I)^2\coth(eV/k_BT)$, while the lower dashed line is the mixed-down noise predicted by Eq. (3.2) in the absence of zero point fluctuations, $(4eV/R)(I_o/I)^2[\exp(2eV/k_BT) - 1]^{-1}$. The small discrepancies between the data and Eq. (1.5) at very low voltages are possibly due to our neglect of noise rounding in the theory. It is evident from Fig. 4 that both the total measured noise across the junction and the measured mixed-down noise are in excellent agreement with the theory that includes a contri-

bution from the mixed-down zero point fluctuations, and are substantially higher than the predictions of a theory that does not include this contribution.

In Fig. 5 we show the temperature dependence of the noise for twelve bias voltages ranging from 50 μV to 550 μV. The notation is the same as that in Fig. 4. The temperature $T = 2eV/k_B$ is indicated for the six lowest voltages; mixed-down noise at temperatures well above this temperature is in the classical limit $eV \ll k_B T$, while that at temperatures well below this temperature is in the quantum limit $eV \gg k_B T$. The mixed-down noise at the six highest voltages is in the quantum limit at all temperatures measured. For all twelve voltages, the total junction noise is in good agreement with the predictions of Eq. (1.5), and substantially greater than the predictions of Eq. (3.2). The data at 300 μV, however, lie somewhat above the prediction. This discrepancy arises from the structure at 300 μV (see Fig. 3) that increases the magnitude of the mixed-down noise above the value predicted by Eq. (1.5) (this topic will be discussed in detail in Sec. III.D.). The mixed-down noise at 350 μV and above is independent of temperature, and in excellent agreement with the value of Eq. (1.7), $S_v(0)/R_D^2 = (2eV/R)(I_o/I)^2$. (As the temperature was lowered, I_o increased slightly, giving rise to the slight increase in the mixed-down noise that is evident in both the data and the theoretical prediction.) As the voltage is lowered the mixed-down noise becomes increasingly temperature dependent, and remains in good agreement with the predictions of Eq. (1.5). At 50 μV, the mixed-down noise is in the classical limit for the whole temperature range, and proportional to T, as expected. This temperature dependence demonstrates that the contribution of any ex-

traneous noise was negligible.

We can extract from our data the measured spectral density of the current noise $S_I(\nu)$ generated by the shunt resistance R at the Josephson frequency $\nu = 2eV/h$. We divide each value of the mixed-down noise by the mixing coefficient $(I_o/I)^2/2$, a procedure that converts the mixed-down noise in Eq. (1.5) into Eq. (1.4). The results are plotted in Fig. 6 for 4.2K (solid circles) and 1.6K (open circles). The solid lines are the corresponding predictions of Eq. (1.4) using measured values of $\nu = 2eV/h$, R, and T. The slight increase of the data above the theory at the highest voltages may reflect the presence of a resonance on the I-V characteristic. The agreement between the data and the predictions is rather good, bearing in mind that, once again, no fitting parameters are used. By contrast, the dashed lines represent the theoretical prediction in the absence of the zero point term, $(4h\nu/R)[\exp(h\nu/k_BT) - 1]^{-1}$, and fall far below the data at the higher frequencies. The existence of zero point fluctuations in the measured spectral density of the current noise is rather convincingly demonstrated.

C. Junction 3

An alternative means of varying the mixed-down noise between the quantum and thermal limits is to change I_o at fixed temperature. The critical current was lowered by trapping flux in the junction. The 1/f noise in junction 3 at 183 kHz was insignificant (< 2%), but the heating correction at the higher voltages was substantial, so that it was necessary to correct the mixed-down noise in addition to the noise generated at the measurement frequency. In Fig. 7 we plot $S_v(0)/R_D^2$ vs. V at 4.2K for four values of I_o corresponding to values of κ ranging from 0.65 to

0.07. At the highest two values of I_o, the presence of a resonance near 200 μV increased the magnitude of the measured noise somewhat above the prediction of Eq. (1.5). Apart from this discrepancy, the measured total noise and the measured mixed-down noise are in very good agreement with the predictions. For $\kappa = 0.65$, the data lie convincingly above the theory that does not include the mixed-down zero point fluctuations, while for $\kappa = 0.07$ the contribution of the zero point term is less than our experimental error. Once again, the correct observed dependence of the noise on I_o demonstrates the absence of any significant extraneous noise.

D. Junction 4

As noted earlier, some junctions contain resonances that can affect the magnitude of the noise mixed down to the measurement frequency. Junction 4 exhibited strong resonant structure, and we have investigated its origin and its effect on the noise in some detail. Figure 8 shows the I-V and (dV/dI) - V characteristics at 1.1K for four values of critical current; the three lowest values were obtained by trapping flux in the junction. The structure arises from the resonant circuit formed by the shunt inductance, L_s, and junction capacitance, C; the equivalent circuit is shown in the inset in Fig. 9. The resonant circuit pulls the Josephson frequency slightly so that it becomes more closely a subharmonic of the resonant frequency. Hence, as the current bias is increased, the dynamic resistance will be alternately increased and decreased as the Josephson frequency passes through each subharmonic frequency of the LCR resonance. The 1/n dependence of the dynamic resistance is shown clearly in Figs. 8 and 9 (n is an integer).

The equations of motion are

$$I = I_o \sin\delta + C\dot{V} + I_s \ , \tag{3.3}$$

and

$$V = I_s R + \dot{I}_s L_s + V_N \ , \tag{3.4}$$

where I_s is the current flowing through the shunt, and V_N is the equilibrium noise voltage generated by R with spectral density $2h\nu R\coth(h\nu/2k_BT)$. We have computed the I-V characteristics and the spectral density of the voltage noise across the junction, using the procedure outlined in the Appendix. To obtain these curves, it was necessary to fit the values of L_s and C. From our simulations, we conclude that the I-V characteristic will show substantial resonant structure when $\beta_L = 2\pi L_s I_o/\Phi_o \gtrsim 0.5$ and the approximate Q of the LCR circuit $(\beta_L/\beta_c)^{\frac{1}{2}} \gg 1$. The observed rapid decrease in the magnitude of the resonant structure as I_o is lowered is demonstrated in Fig. 8.

Figure 9 shows I and R_D vs. V for junction 4 at 1.4K, the temperature at which the noise measurements were made. The computed dynamic resistance is also shown, using L_s = 0.23 pH and C = 0.81 pF; these values are consistent with values expected from the dimensions of the sample. The agreement between the measured and computed values is quite good, although the measured structure at the higher voltages is considerably more smeared than predicted, possibly because of noise rounding. Furthermore, the measurements lie slightly below the computed values at lower voltages, even though noise rounding is negligible in this region. This discrepancy occurs because the measured shunt resistance at low voltages dropped somewhat below the

high voltage value, a fact that could not readily be included in the computer simulation (see Appendix).

This junction was investigated at an early stage of our work, and we measured the noise mostly at one frequency only, 98.6 kHz, with a few measurements at 31.6 kHz. We used the following procedure to subtract the 1/f noise in the range of voltage where the oscillations occured. First, if the 1/f noise arises from fluctuations in the critical current,[21] the spectral density of the voltage noise should be proportional to $(\partial V/\partial I_o)^2$. At voltages where the RSJ result, Eq. (1.2), is valid we find

$$\left(\frac{\partial V}{\partial I_o}\right)^2 = R^2\left(\frac{I_o R}{V}\right)^2 . \tag{3.5}$$

Hence, the voltage noise arising from 1/f fluctuations will be

$$S_V^{1/f}(\nu) = R^2(I_o R/V)^2 S_{I_o}^{1/f}(\nu) , \tag{3.6}$$

where $S_{I_o}^{1/f}(\nu)$ is the spectral density of the 1/f fluctuations in the critical current at the measurement frequency. Second, the mixed-down noise in Eq. (1.1) for voltages well below $k_B T/e$ can be written as $(2k_B TR)(I_o R/V)^2$. Thus, at low voltages where the deviations from the RSJ model are negligible and for fixed values of I_o, R and T, the spectral densities of both the mixed-down noise and 1/f noise (and their sum) should be proportional to $1/V^2$. Figure 10 shows the spectral densities of the voltage noise across the junction for V < 100 μV at 98.6 kHz, and for two voltages at 31.6 kHz, with the direct term $(4k_B T/R)R_D^2$ subtracted out. At 98.6 kHz the plotted quantity scales with $1/V^2$, suggesting that the 1/f noise scales as $(\partial V/\partial I_o)^2$. We then assume that the spectral density of the excess noise scales as 1/f,

and from data at the two voltages where measurements were made at two frequencies, calculate the spectral density of the 1/f noise in the critical current: $S_{I_o}^{1/f}(98.6\ \text{kHz}) = 5.5 \times 10^{-22}\ A^2Hz^{-1}$. By subtracting the 1/f voltage noise computed using Eq. (3.6) from the data at 98.6 kHz, we obtain the mixed-down noise shown in Fig. 10. The mixed-down noise is in excellent agreement with the predicted value. Thus, this procedure provides strong evidence that the spectral density of the excess noise at low voltages scales closely as 1/f (as is the case for all junctions on which we have measurements at three frequencies). We then calculated the 1/f voltage noise at the higher voltages (> 100 μV) from measurements at 98.6 kHz, using the value of $S_{I_o}^{1/f}$ quoted above, together with measured values of $\partial V/\partial I_o$. We also measured the noise at 31.6 kHz at several voltages between 100 and 200 μV, and obtained values that were consistent with those obtained by the above procedure. Since the overall 1/f correction was small, typically 15% or less of the total junction noise at 200 μV, we believe that the error introduced by the correction is at most ± 5% of the mixed-down noise.

As a further complication, we did not measure the heating correction on this junction, but rather on one fabricated simultaneously. As a result the heating correction had a higher uncertainty, which we estimate to be ± 6% of the total spectral density, than for the other junctions.

Figure 11(a) shows the spectral density of the measured voltage noise at 1.4K, together with the measured mixed-down noise computed by subtracting $4k_BTR_D^2/R$, with the 1/f noise subtracted. The solid line shows the result of the computer simulation, with the zero point term included and with the values of L_s and C obtained by fitting the model to the I-V characteristics in Fig. 10. The data tend to lie somewhat above the computed curve at voltages above 100 μV. In Fig. 11(b) we have applied a heating correction by subtracting $4k_B\Delta TR_D^2/R$ from the solid circles in 11(a). The

agreement between the measured and computed values is now rather good, indicating that our model is a good approximation.

Our computer simulation yields the magnitudes of the contributions of the noise generated at multiples of the Josephson frequency, as shown in Fig. 12. We define a mixing impedance,[8] Z_k, via the relation

$$S_v(0) = \sum_{k=0}^{\infty} S_v^{(k)}(0) = \sum_{k=0}^{\infty} |Z_k|^2 S_I(k\nu_J) \ , \qquad (3.7)$$

where k = 0, 1, 2 ..., and $S_v^{(k)}(0)$ is the spectral density of the mixed-down voltage noise due to noise near frequency $k\nu_J$. We note that $|Z_o|^2 = R_D^2$. For $\beta_c = 0.031$ and $\beta_L = 0.05$, Z_k is essentially zero for $k \geqslant 2$, and the deviations from the RSJ model are negligible. On the other hand, for $\beta_L = 0.4$ and 1.05, there are very substantial contributions to the noise from harmonics out to the 5th and 9th, respectively, and the noise is considerably enhanced over the value predicted by Eq. (1.5). These results explain quantitatively the additional noise associated with the resonant structure, and, qualitatively, the additional noise observed on junctions 2 and 3 in the vicinity of structure on the I-V characteristic. In fact, the capacitance and inductance of these two junctions were estimated from computer fits to this structure.

Although the data obtained from junction 4 are considerably harder to interpret than those from the other junctions, the role of zero point fluctuations is even more important because of the large number of harmonics that contribute to the mixed-down noise. The noise generated at frequencies near the higher harmonics can be in the quantum limit even for junctions with $\kappa < 1$.

IV. CONCLUDING REMARKS

We emphasize that in comparing the data for junctions 1, 2, and 3 with theory we have used only measured parameters; there is no fitting of the data. Thus, junctions 2 and 3 provide the main evidence for the accuracy of Eq. (1.5). We believe the results obtained from these junctions are a convincing demonstration first, of the existence of a zero point term in the spectral density of the current noise of a resistor in thermal equilibrium (Fig. 6), and, second, that these fluctuations give rise to the limiting voltage noise in a current-biased resistively shunted Josephson junction in the quantum limit for $I > I_o$ (Figs. 4, 5, and 7). Furthermore, the good agreement between our results and Eq. (1.5) justifies our use[14] of a Langevin equation together with a zero-point driving term to predict quantum noise effects in a current-biased Josephson junction in the overdamped limit when it is in the free-running mode $I > I_o$. We were not able to examine the validity of the theory in the noise-rounded case $I < I_o$ since quantum effects are negligible in this regime in the He^4 temperature range for the parameters of our junctions.

The data from junction 4, which exhibited resonant structure, require a fitting of L_s and C to compare the experimental results with the theory. However, we note that the values of L_s and C that yield an excellent fit to the measured I and dV/dI vs. V characteristics, also produce a very good fit to the noise data (Fig. 11). These results show very dramatically the strong effects of additional non-linearities on the voltage noise due to the mixing-down of higher order harmonics. Because quantum effects increase rapidly as the order of the harmonic increases, the role of zero point fluctuations is even more pronounced in junctions with re-

sonant structure.

The fact that the zero point fluctuations in the resistor can be observed at frequencies as high as 5×10^{11} Hz implies that a Josephson mixer using the ac Josephson effect as the local oscillator is an ideal quantum-limited device at these frequencies. When an external local oscillator is used, however, the additional non-linearity induced on the I-V characteristic causes noise near the higher harmonics of the Josephson frequency to be mixed down, thereby greatly increasing the noise of the mixer. This limitation of the Josephson mixer with an external local oscillator has been discussed extensively by other authors.[22,23]

Finally, in accord with other observations,[24,25] we find no evidence for a contribution to the measured noise arising from the shot noise of pairs tunneling through the junction. For example, in Fig. 4, the spectral density of a term $4eI_o$ would be about 3.2×10^{-22} A^2Hz^{-1}, a value at least five times greater than the observed mixed-down noise at 1 mV. We emphasize, however, that this observation in no way invalidates the theory of Stephen,[12] which is applicable to a quite different situation.

ACKNOWLEDGMENTS

R. H. Koch and D. J. Van Harlingen would like to thank the National Science Foundation for pre- and post-doctoral fellowships. We should like to thank Dr. J. H. Greiner and Dr. L. D. Jackel and his colleagues for helpful discussions on junction fabrication. We are indebted to the Micro Electronics Facility in the Electronics Research Laboratory of the Electrical Engineering and Computer Science Department at U.C. Berkeley for the use of their facilities. This work was supported by the Director, Of-

fice of Energy Research, Office of Basic Energy Sciences, Materials Sciences Division of the U.S. Department of Energy under Contract No. W-7405-ENG-48.

APPENDIX. TWO METHODS OF COMPUTING I-V CHARACTERISTICS AND NOISE IN RESISTIVELY SHUNTED JUNCTIONS

In this appendix, we outline two methods of computing the I-V characteristics and spectral density of the voltage noise for resistively shunted junctions. The first method calculates the I-V characteristics and R_D, including noise-rounding, and can also be used to compute the spectral density of the voltage noise, although the last calculation is rather slow. Unfortunately, for reasons that we will explain, this method is not useful for computing the noise in a junction with resonant structure, such as junction 4. The second method calculates the noise very efficiently at voltages where noise rounding is negligible. With the model of the junction we have used, this method appears to account for most of the data observed on junction 4 satisfactorily, although higher order corrections might provide a better fit at voltages above, say 500 μV.

Method 1

The model circuit, inset in Fig. 9, is described by Eqs. (3.3) and (3.4). We rewrite these equations in dimensionless units $v = V/I_oR$, $i = I/I_o$, $s = I_s/I_o$, and $\theta = t/(\Phi_o/2\pi I_oR)$, and use ω as a dimensionless angular frequency to obtain:

$$i = \sin\delta + \beta_c\ddot{\delta} + s \qquad \text{(A1)}$$

and

$$\dot{\delta} = s + \beta_L\dot{s} + v_n \ , \qquad \text{(A2)}$$

where $\dot{\delta} \equiv \partial\delta/\partial\theta$, etc., and we have used $2eV = \hbar\partial\delta/\partial t$. As usual, $\beta_c \equiv 2\pi I_o R^2 C/\Phi_o$ and $\beta_L \equiv 2\pi L_s I_o/\Phi_o$. The instantaneous state of the junction is specified completely by $\dot{\delta}$, δ and s. Using Eqs. (A1) and (A2) one can compute $\dot{s}$ and $\ddot{\delta}$ and the higher order derivatives of δ and s, for example:

$$\beta_L \ddot{s} = \ddot{\delta} - \dot{s} \ , \tag{A3}$$

$$\beta_c \dddot{\delta} = - \ddot{\delta} \cos\delta - \dot{s} \ , \tag{A4}$$

and so on. We have neglected all derivatives of v_n. Once the derivatives have been evaluated numerically for the existing values of δ, $\dot{\delta}$, and s at time θ, we compute the new values δ_1, $\dot{\delta}_1$, and s_1 at a later time, $\theta + \tau$, by using a fifth-order Taylor expansion:

$$\delta_1 = \delta + \dot{\delta}\tau + \ldots + (\partial^5\delta/\partial\theta^5)\tau^5/5! \ , \tag{A5}$$

$$\dot{\delta}_1 = \dot{\delta} + \ddot{\delta}\tau + \ldots + (\partial^5\delta/\partial\theta^5)\tau^4/4! \ , \tag{A6}$$

and

$$s_1 = s + \dot{s}\tau + \ldots + (\partial^5 s/\partial\theta^5)\tau^5/5! \ . \tag{A7}$$

To predict the average voltage for $i > 1$, we set $v_n = 0$, integrate Eqs. (A1) and (A2) numerically over exactly one Josephson cycle, measure the required time θ, and compute $\langle v \rangle = \langle \dot{\delta} \rangle = 2\pi/\theta$. This procedure was used to compute the values of R_D in Fig. 9, with values of L_s and C chosen to

fit the data.

The results were independent of the length of the time step, τ, provided τ was less than the smaller of β_c or β_L. To check that the presence of noise did not affect the characteristics for $i > 1$, we varied v_n in time to simulate noise from the resistor while the junction was allowed to evolve over many Josephson cycles. The resulting values of the voltage were identical to those with $v_n = 0$.

To obtain a time-representation of $v_n(\theta)$ with a white power spectrum, $S_v^w(\omega)$, we used a pseudorandom number generator to produce voltage pulses that were gaussian distributed in amplitude and uncorrelated in time. A non-white power spectrum, $S_v^{nw}(\omega)$, could be generated, when necessary, by convolving this time representation with an appropriate filter function. This filter function was chosen so that its transfer function in the frequency domain, $T(\omega)$, satisfied

$$S_v^{nw}(\omega) = |T(\omega)|^2 S_v^w(\omega) \quad . \tag{A8}$$

The high-frequency cut-off, ω_H, of $v_n(\theta)$ was always chosen to be large enough that the predicted average voltage and noise voltage were independent of the value of ω_H when the latter was varied over a factor of 20 or more. Furthermore, when the noise near the Josephson frequency was non-white, we took account of the implied non-zero correlation time by ensuring that the correlation time of the filter was much larger than $1/\nu_J$.

To obtain $\langle\dot{\delta}\rangle$, the computed values of $\dot{\delta}(\theta)$ were filtered with a low-pass gaussian filter with a roll-off frequency, ω_L, of 0.03 to 0.1 ν_J. The fluctuations in the filtered values of $\langle\dot{\delta}\rangle$ were used to compute the low

frequency spectral density of the voltage noise. This spectral density was independent of the roll-off frequency of this low-pass filter.

This method was used in two earlier papers[15,26] to predict $\langle\dot{\delta}\rangle$ and the fluctuations in $\dot{\delta}$ in single junctions and dc SQUIDs, including low-voltage regions of the I-V characteristics where there is significant noise rounding. However, when we tried to use this method to predict the noise in junction 4, which has substantial resonant structure, we obtained very poor results. The essential problem was that the resonant frequency, $\omega_{LC} = (L_s C)^{-\frac{1}{2}}$, was typically 5 to 20 times higher than ω_J, while ω_H was necessarily at least several times greater than ω_{LC}. Thus, since ω_L was typically an order of magnitude less than ω_J the ratio of ω_H/ω_L was typically 10^3. Consequently, the ratio of the "input" noise power to the "output" noise power for "f-noise" was typically 10^6. The computed spectral densities of the noise proved to be erratic with such large ratios, possibly because of our neglect of the derivatives of v_n in Eq. (A3). As a result, we had to abandon this technique for junctions with resonant structure.

Method 2

Above the noise-rounded region of the I-V characteristic, we used a more accurate but more complicated method to calculate the noise in resonant junctions. In this region, following the perturbation approach of Likharev and Semenov,[8] we can expand δ and s:

$$\delta(\theta) = \delta_o(\theta) + \tilde{\delta}(\theta) \tag{A9}$$

and

$$s(\theta) = s_o(\theta) + \tilde{s}(\theta) \ , \tag{A10}$$

where δ_o and s_o are the noise-free solutions for the phase and shunt current, and $\tilde{\delta}$ and $\tilde{s}$ represent small departures from δ_o and s_o due to noise. Substituting these expressions into Eqs. (A1) and (A2), we find

$$0 = \tilde{\delta} \cos\delta_o + \beta_c \ddot{\tilde{\delta}} + \tilde{s} \tag{A11}$$

and

$$\dot{\tilde{\delta}} = \tilde{s} + \beta_L \dot{\tilde{s}} + v_n \ . \tag{A12}$$

We Fourier transform these equations over the range $-\infty < \omega < \infty$ to obtain

$$0 = \int_{-\infty}^{\infty} F(\omega')\tilde{\delta}(\omega - \omega')d\omega' + \beta_c(-\omega^2)\tilde{\delta}(\omega) + \tilde{s}(\omega) \tag{A13}$$

and

$$j\omega\tilde{\delta}(\omega) = (1+j\omega\beta_L)\tilde{s}(\omega) + v_n(\omega) \ , \tag{A14}$$

where $F(\omega')$ is the normalized Fourier transform of $\cos\delta_o(\theta)$. Since $\cos\delta_o(\theta)$ is a periodic function, $F(\omega')$ consists of a series of spiked functions centered at $\omega = 0$ and spaced at invervals of ω_J. Setting $\omega' = k\omega_J$, where k is an integer, we can transform the integral to a sum, replace $F(k\omega_J)$ with F_k, and

eliminate s between Eqs. (A13) and (A14) to find

$$\sum_{k=-\infty}^{\infty} F_k \tilde{\delta}(\omega - k\omega_J) + \left(\frac{j\omega}{1 + j\omega\beta_L} - \omega^2 \beta_c \right) \tilde{\delta}(\omega) = \frac{v_n(\omega)}{1 + j\omega\beta_L} . \qquad \text{(A15)}$$

In subsequent calculations, we have shown that there exists a maximum value of $|k|$, k_m, above which the noise at frequency $k\omega_J$ is not significantly mixed down to the measurement frequency. Cutting off the summation at $\pm k_m$, we are left with $2k_m + 1$ inhomogeneous equations with unknown phases $\tilde{\delta}(\omega - \ell_m\omega_J)$, ..., $\tilde{\delta}(\omega + \ell_m\omega_J)$, where $|\ell| \leq k_m$. To solve these, we first compute the coefficients F_k using method 1 (with $v_n = 0$). The required fluctuations in the $\tilde{\delta}(\omega - \ell\omega_J)$ are then obtained by a conventional matrix inversion of Eq. (A15). We find

$$\tilde{\delta}(\omega + \ell\omega_J) = \sum_{k=-k_m}^{+k_m} \frac{A_{\ell,k}\, v_n(\omega + k\omega_J)}{1 + j(\omega + k\omega_J)\beta_L} , \qquad \text{(A16)}$$

where $\bar{\bar{A}} \equiv \bar{\bar{B}}^{-1}$, and $\bar{\bar{B}}$ is the matrix representation of Eq. (A15):

$$\{\bar{\bar{B}}\}_{\ell,k} = F_{\ell-k} + \delta_{\ell,k}\left[\frac{j(\omega + \ell\omega_J)}{1 + j(\omega + \ell\omega_J)\beta_L} - (\omega + \ell\omega_J)^2 \beta_c \right] . \qquad \text{(A17)}$$

In Eq. (A17), $\delta_{\ell,k}$ is the Kronecker delta. Since the v_n at different frequencies are independent, the noise at the measurement frequency can be obtained from Eq. (A16) with $|\omega| \ll |\omega_J|$ and $\ell = 0$:

$$s_\delta^*(\omega) = \sum_{k=-k_m}^{k_m} |z_k(\omega)|^2 s_i(\omega + k\omega_J), \qquad \text{(A18)}$$

where

$$z_k(\omega + \ell\omega_J) = \frac{j(\omega + \ell\omega_J)A_{\ell,k}}{1 + j(\omega + k\omega_J)\beta_L}, \qquad (A19)$$

is the complex dimensionless impedance that mixes noise from $(\omega + k\omega_J)$ to $(\omega + \ell\omega_J)$, and $s_i(\omega + k\omega_J)$ is the dimensionless spectral density of the noise current in the resistor. We obtain Eq. (3.7) from Eq. (A18) by replacing ω with ν, setting $\nu = 0$, using positive frequencies only, and assigning appropriate dimensions. In dimensioned units, at frequencies small compared with Z_o/L_s, Z_o is just the dynamic resistance. Thus, the method can be tested by comparing the value of Z_o with the value of R_D obtained with method 1. The computed values of $z(\omega)$ were shown to be independent of ω for $\omega \ll \omega_J$, and ω/ω_J was chosen to be between 1/30 and 1/10. The value of k_m, typically 16 to 25, was chosen so that $k_m\omega_J \gg \omega_{LC}$; the value of k_m was varied to show that the values of $Z(\omega)$ did not depend on it.

The method was used to compute the spectral density of junction 4 shown in Fig. 11, and the corresponding values of $|Z_k|^2$ in Fig. 12. The complexity of the method does not easily allow the value of R to be voltage dependent, and the noise in Fig. 11 was computed with R = 0.092 Ω for all voltages. This approximation gave rise to the discrepancy between the measured and predicted noise at low voltages in Fig. 11.

REFERENCES

*Present address: Department of Physics and Materials Research Laboratory, University of Illinois at Urbana-Champaign, Urbana, Illinois 61801.

1. W. C. Stewart, Appl. Phys. Lett. 12, 277 (1968).

2. D. E. McCumber, J. Appl. Phys. 39, 3113 (1968).

3. B. D. Josephson, Phys. Lett. 1, 251 (1962).

4. V. Ambegoakar and B. I. Halperin, Phys. Rev. Lett. 22, 1364 (1969).

5. A. N. Vystavkin, V. N. Gubankov, L. S. Kuzmin, K. K. Likharev, V. V. Migulin, and V. K. Semenov, Phys. Rev. Appl. 9, 79 (1974).

6. J. Kurkijärvi and V. Ambegoakar, Phys. Lett. 31A, 314 (1970).

7. R. F. Voss, J. Low Temp. Phys. 42, 151 (1981).

8. K. K. Likharev and V. K. Semenov, Pis'ma Zh. Eksp. Teor. Fiz. 15, 625 (1972) [JETP Lett. 15, 442 (1972)].

9. R. H. Koch and J. Clarke (unpublished).

10. C. M. Falco, W. H. Parker, S. E. Trullinger, and P. K. Hansma, Phys. Rev. B 10, 1865 (1974).

11. R. J. Soulen, Jr. and R. P. Giffard, Appl. Phys. Lett. 32, 770 (1978).

12. M. J. Stephen, Phys. Rev. 182, 531 (1969).

13. A. J. Dahm, A. Denenstein, D. N. Langenberg, W. H. Parker, D. Rogovin, and D. J. Scalapino, Phys. Rev. Lett. 22, 1416 (1969).

14. R. H. Koch, D. J. Van Harlingen, and J. Clarke, Phys. Rev. Lett. 45, 2132 (1980).

15. H. B. Callen and T. A. Welton, Phys. Rev. 83, 34 (1951).

16. Yu. M. Ivanchenko and L. A. Zil'berman, Zh. Eksp. Teor. Fiz. 55, 2395 (1968) [Sov. Phys. JETP 28, 272 (1969)].

17. A. J. Leggett, J. de Phys. C6, 1264 (1978).

18. J. Kurkijärvi, Superconducting Quantum Interference Devices and their Applications (Ed. H. D. Hahlbohm and H. Lübbig, Walter de Gruyter, Berlin, 1980), p.247.

19. A. O. Caldeira and A. J. Leggett, Phys. Rev. Lett. 46, 211 (1981).

20. J. H. Greiner, C. J. Kircher, S. P. Klepner, S. K. Lahiri, A. J. Warnecke, S. Basavaiah, E. T. Yen, John M. Baker, P. R. Brosious, H.-C. W. Huang, M. Murakami, and I. Ames, IBM J. of Res. and Dev. 24, 195 (1980).

21. J. Clarke and G. Hawkins, Phys. Rev. B 14, 2826 (1976).

22. J. H. Claassen and P. L. Richards, J. Appl. Phys. 49, 4117 (1978).

23. Y. Taur, IEEE Trans. Electron Devices ED-27, 1921 (1980).

24. J. H. Claassen, Y. Taur, and P. L. Richards, Appl. Phys. Lett. 25, 759 (1974).

25. R. P. Giffard, P. F. Michelson, and R. J. Soulen, IEEE Trans. Magn. MAG-15, 276 (1979).

26. R. H. Koch, D. J. Van Harlingen, and J. Clarke, Appl. Phys. Lett. 38, 380 (1981).

TABLE I. Parameters of Junctions[a,b]

Junction	1	2		3	4
Temperature (K)	4.2	4.2	1.6	4.2	1.4
I_o (mA)	0.32	0.51	0.60	0.36	1.53
R (Ω)	0.075	0.67Ω at 50μV		0.58Ω at 50μV	0.084Ω at 50μV
		0.70Ω at 100μV		0.62Ω at 100μV	0.092Ω at 100μV
		0.75Ω at 400μV		0.68Ω at 200μV	
				0.77Ω at 400μV	
β_c	0.003	0.38	0.45	0.21	0.032
β_L	0.20	0.31	0.37	0.22	1.05
κ	0.066	0.99	3.0	0.62	1.17
$S_{I_o}^{1/f}(A^2Hz^{-1})$	$< 2 \times 10^{-22}$	6.0×10^{-23}	3.0×10^{-23}	$< 3 \times 10^{-24}$	5.5×10^{-22}
(frequency)	(100kHz)	(183kHz)	(183kHz)	(183kHz)	(100kHz)
Heating (K/μW)	< 1	0.25	1.6	7	1.6

a C = 0.5 pF for 1, 2, 3, 0.81 pF for 4; R taken at 100μV.

b L = 0.2 pH for 1, 2, 3, 0.23 pH for 4; R taken at 100 μV.

FIGURE CAPTIONS

Fig. 1 (a) Configuration of resistively shunted tunnel junction; (b) Schematic of measuring circuit; the dashed lines enclose the components immersed in liquid helium.

Fig. 2 $S_v(0)$ vs. I for junction 1 at 4.2K. Solid circles are data with dashed line drawn through them; solid line is prediction of Eq. (1.1).

Fig. 3 I and R_D vs. V for junction 2 at 4.2K.

Fig. 4 $S_v(0)/R_D^2$ vs. V for junction 2 at 4.2K. The open circles show the total measured noise across the junction; solid circles below show the noise remaining after correction for 1/f noise and heating. Upper solid and dashed lines are predictions of Eq. (1.5) and (3.2). Solid triangles are measured mixed-down noise, lower solid and dashed lines are mixed-down noise predicted by Eqs. (1.5) and (3.2).

Fig. 5 $S_v(0)/R_D^2$ vs. T for junction 2 at 12 bias voltages. Notation is as for Fig. 4. Arrows indicate $2eV = k_BT$.

Fig. 6 Measured spectral density of current noise in shunt resistor of junction 2 at 4.2K (solid circles) and 1.6K (open circles). Solid lines are prediction of Eq. (1.4), while dashed lines are $(4h\nu/R)[\exp(h\nu/k_BT) - 1]^{-1}$.

Fig. 7 $S_v(0)$ vs. V for junction 3 at 4.2K for 4 values of I_o. Notation is as for Fig. 4.

Fig. 8 I-V and dV/dI-V curves for junction 4 at 1.1K for four values of I_o.

Fig. 9 I and R_D vs. V for junction 4 at 1.4K with I_o = 1.53 mA, R =

0.092Ω, $\kappa = 1.17$, $\beta_L = 1.05$, and $\beta_c = 0.032$. Dashed line is computed R_D. Inset is equivalent circuit of junction.

Fig. 10 Spectral density of total voltage noise across junction 4 at two frequencies in the region $V < k_B T/e$ with $(4k_B T R_D^2/R)$ subtracted out (open and solid circles). Solid lines have slope - 2. Triangles are measured mixed-down noise assuming excess low frequency noise is proportional to 1/f; dashed line is prediction of Eq. (1.1).

Fig. 11 (a) Open circles are measured voltage noise across junction 4 at 1.4K, solid circles are mixed-down noise with 1/f noise subtracted. Solid and dashed lines are predictions of computer simulation with and without zero point term.

(b) Solid circles are data after heating correction has been made, solid line is identical to that in (a).

Fig. 12 $|Z_k|^2/R^2$ for a junction with $\beta_c = 0.031$ for 3 values of β_L and a bias current $I/I_o = 1.42$.

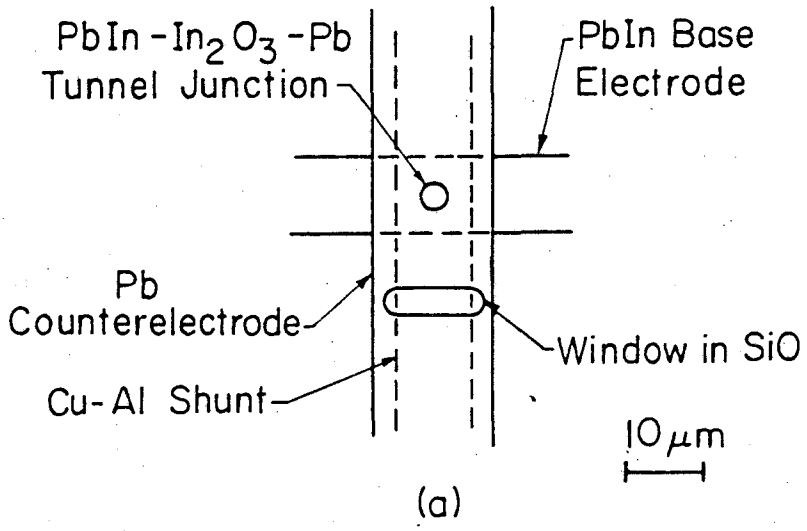

(a)

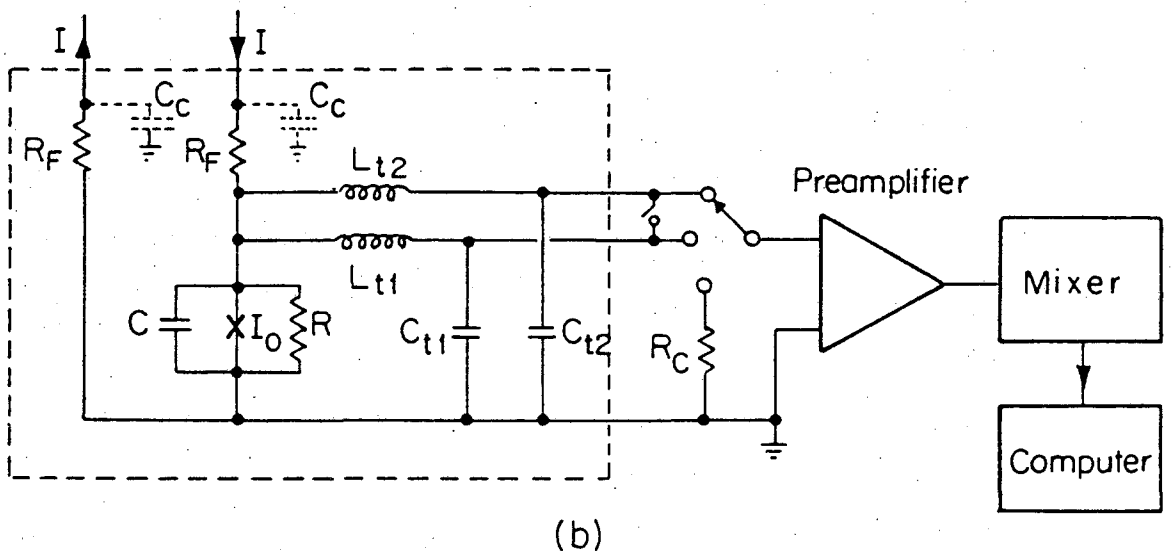

(b)

XBL 818-6303

Fig. 1

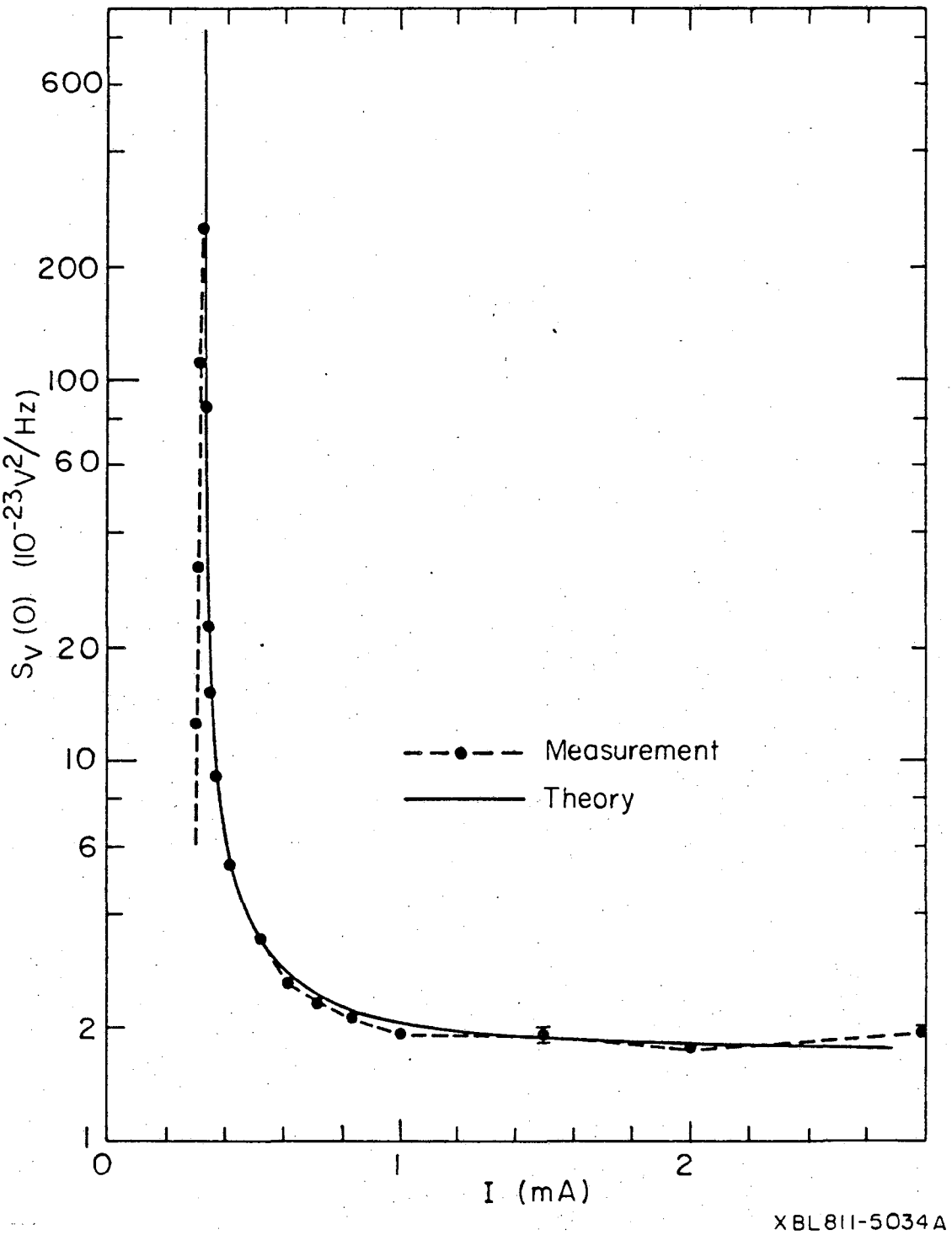
600
200
100
60
20
10
6
2
1
0
1
2
$S_V(0)$ $(10^{-23}V^2/Hz)$
I (mA)
Measurement
Theory
XBL811-5034A

Fig. 2

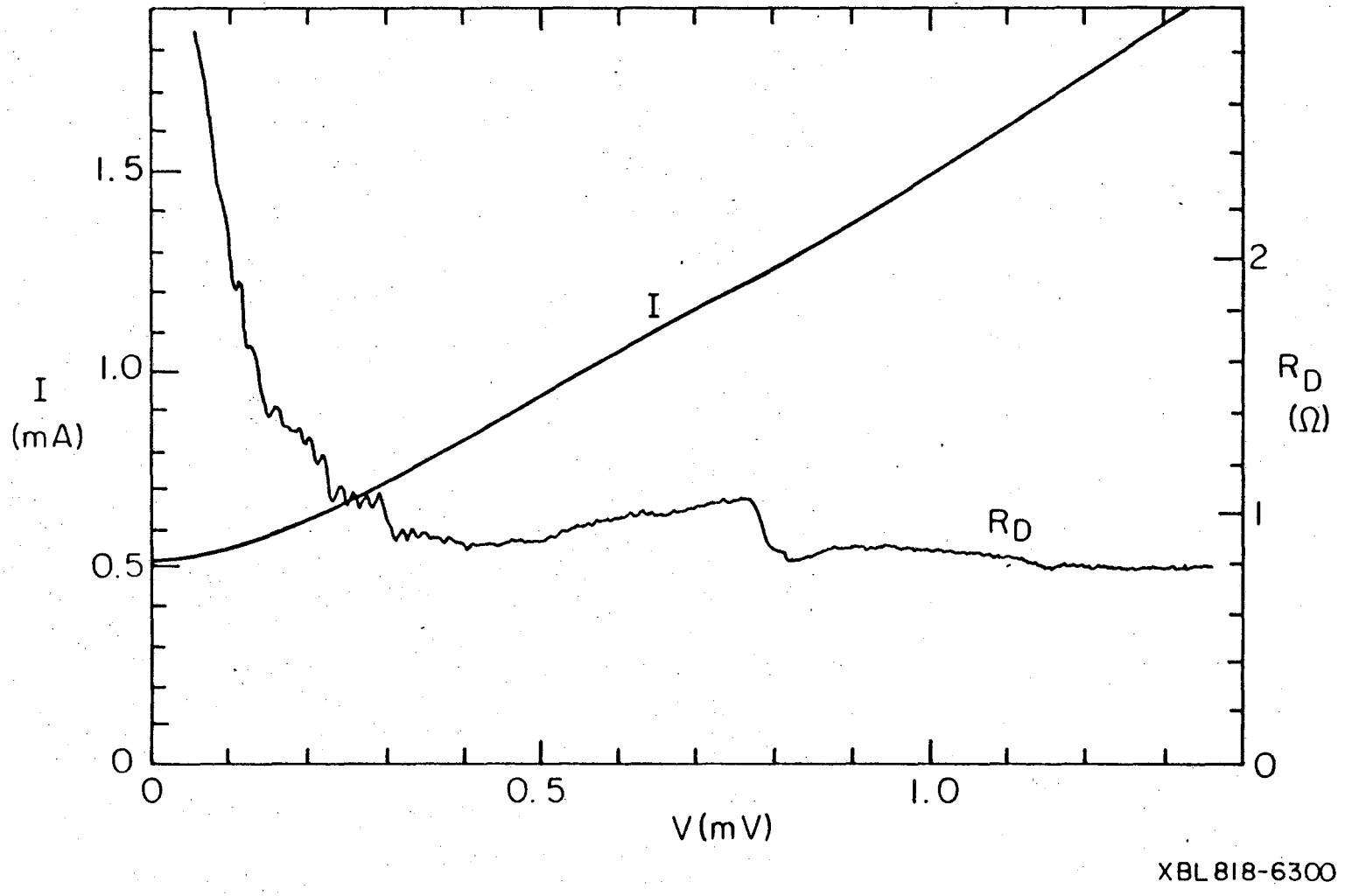

Fig. 3

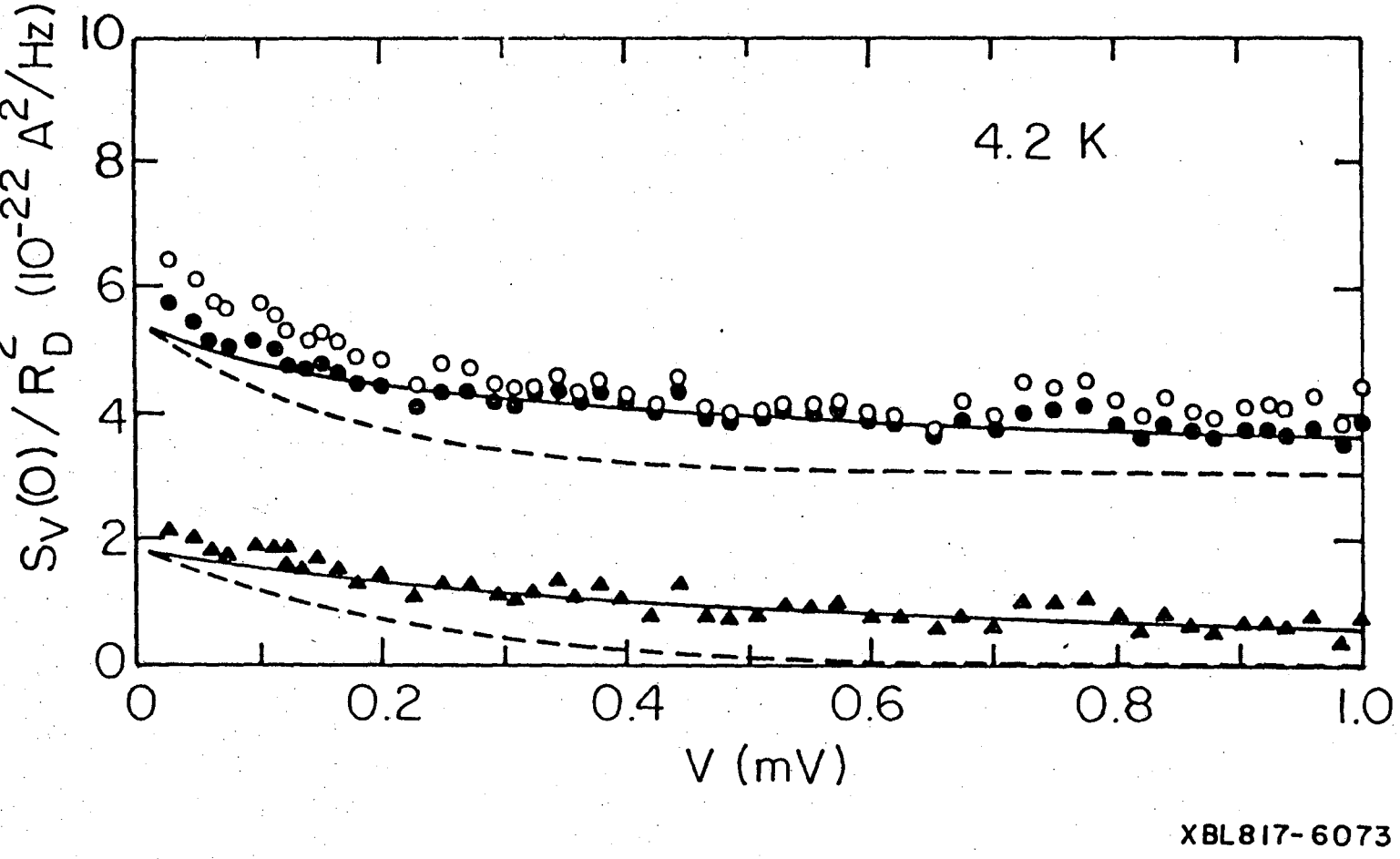

Fig. 4

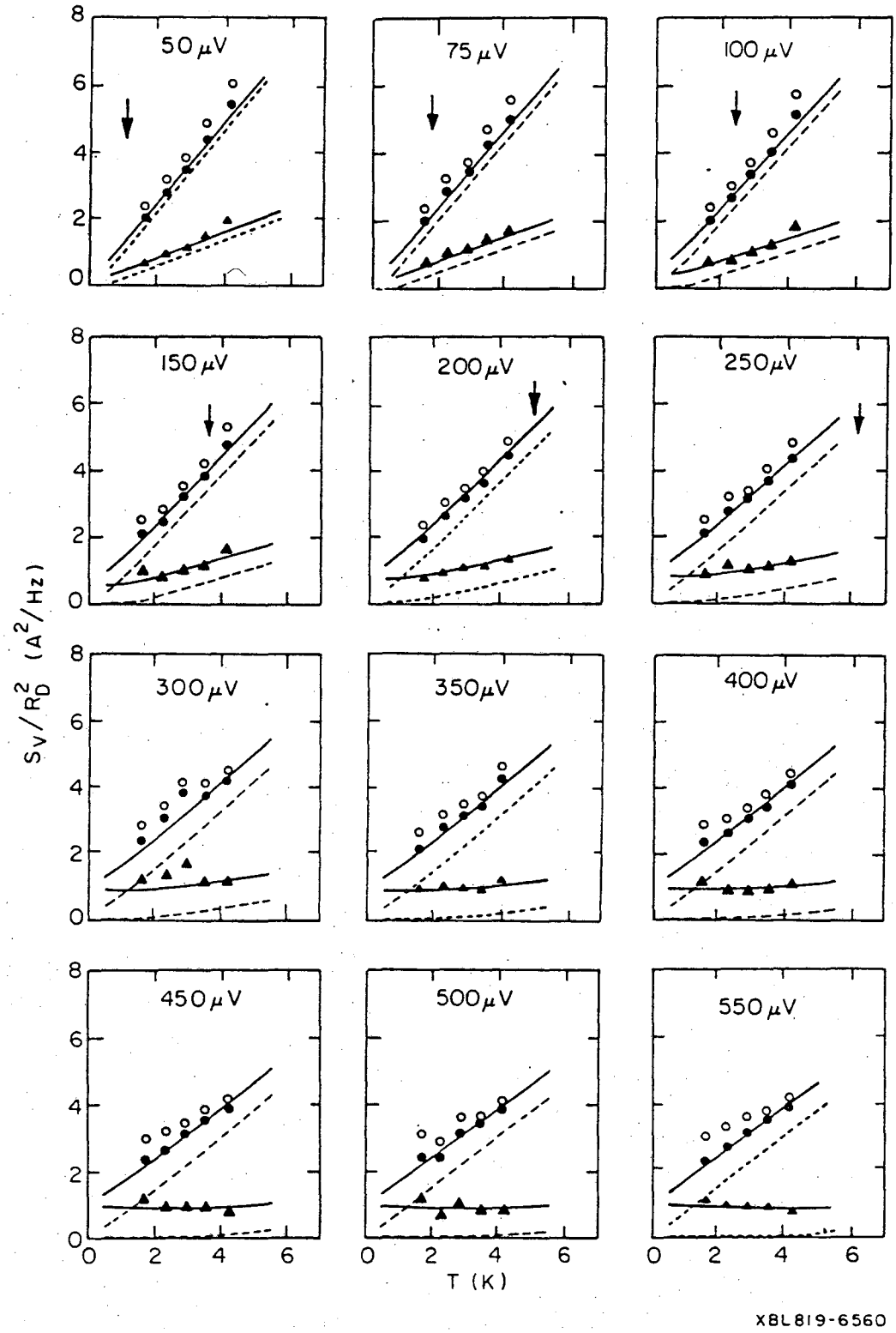
50 μV
75 μV
100 μV
150 μV
200 μV
250 μV
300 μV
350 μV
400 μV
450 μV
500 μV
550 μV
S_V/R_D^2 (A²/Hz)
T (K)
XBL819-6560

Fig. 5

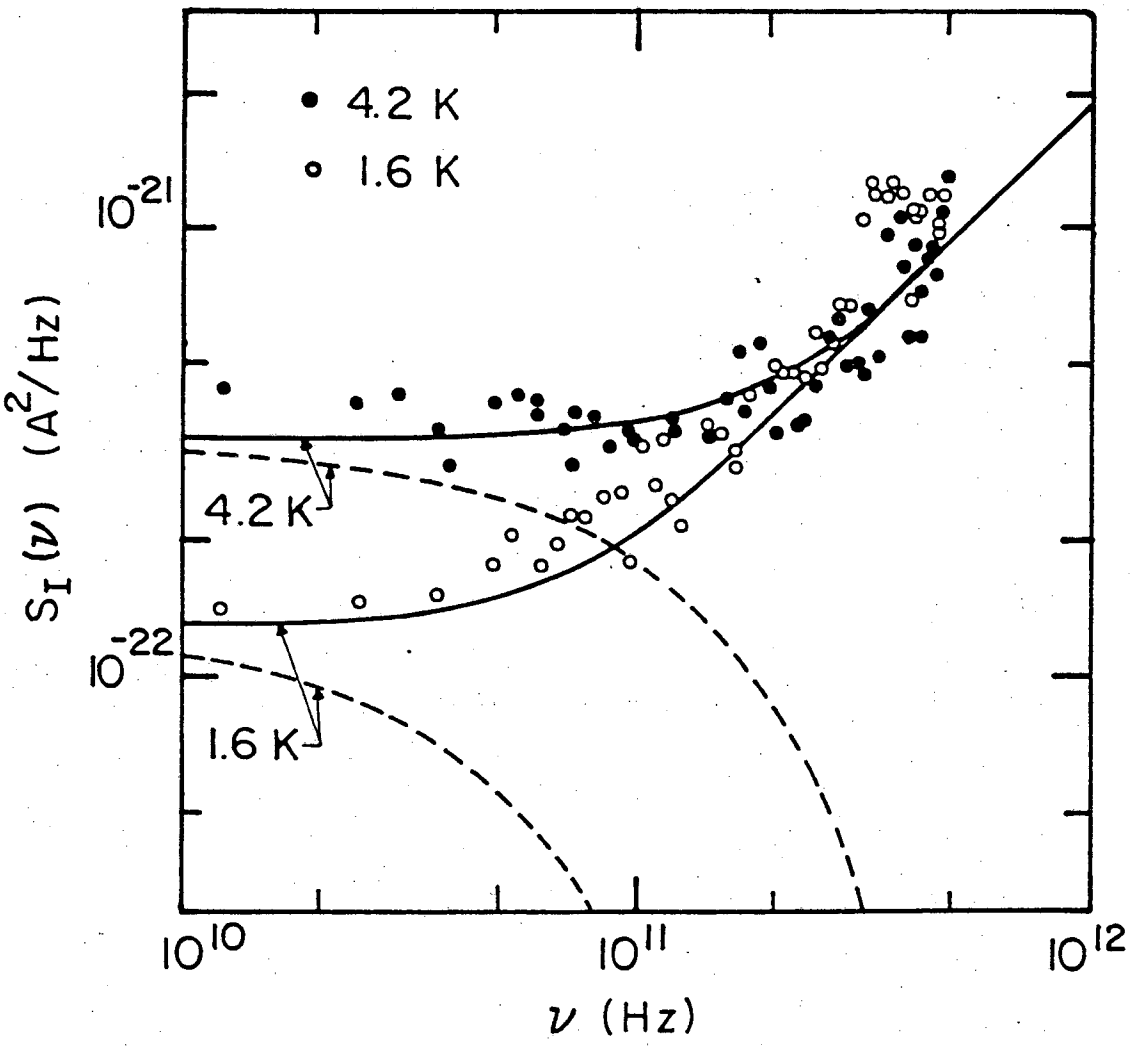

XBL 817-6072

Fig. 6

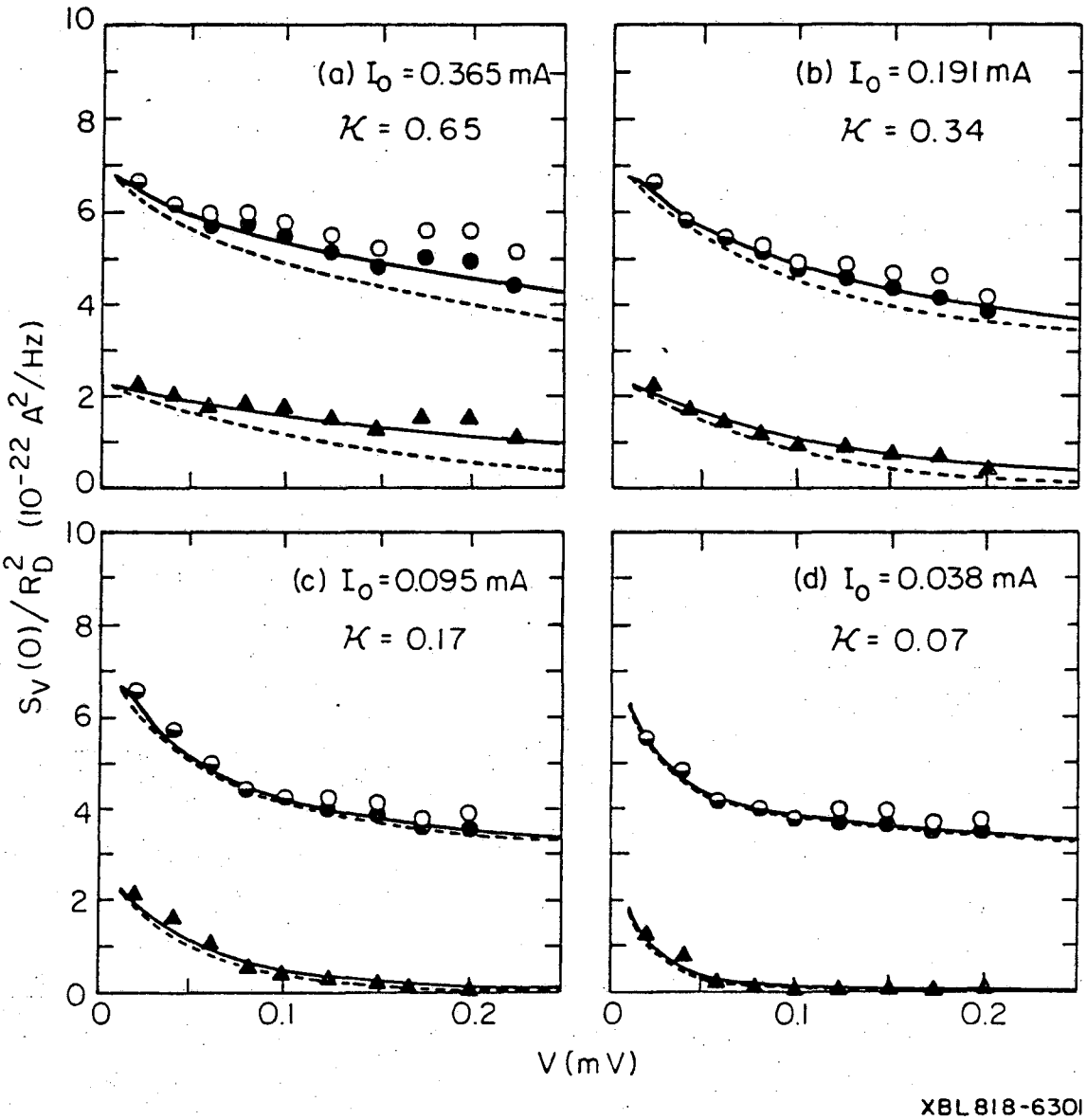
(a) I_0 = 0.365 mA
$\mathcal{K}$ = 0.65
(b) I_0 = 0.191 mA
$\mathcal{K}$ = 0.34
(c) I_0 = 0.095 mA
$\mathcal{K}$ = 0.17
(d) I_0 = 0.038 mA
$\mathcal{K}$ = 0.07
$S_V(0)/R_D^2$ (10^{-22} A^2/Hz)
V (mV)
0
2
4
6
8
10
0.1
0.2
XBL 818-6301

Fig. 7

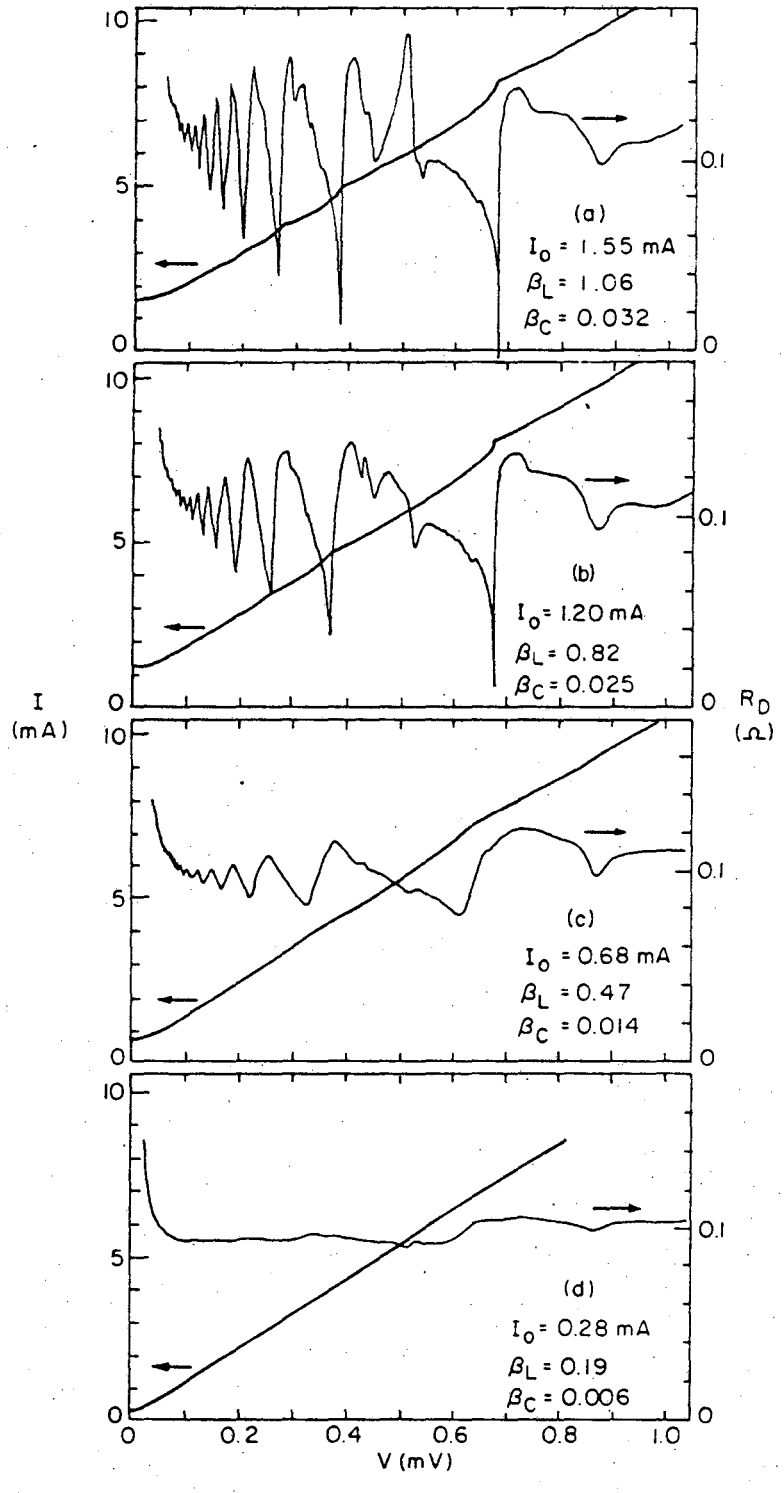
(a)
I_o = 1.55 mA
β_L = 1.06
β_C = 0.032
(b)
I_o = 1.20 mA
β_L = 0.82
β_C = 0.025
(c)
I_o = 0.68 mA
β_L = 0.47
β_C = 0.014
(d)
I_o = 0.28 mA
β_L = 0.19
β_C = 0.006
I (mA)
R_D (Ω)
V (mV)
XBL818-6316

Fig. 8

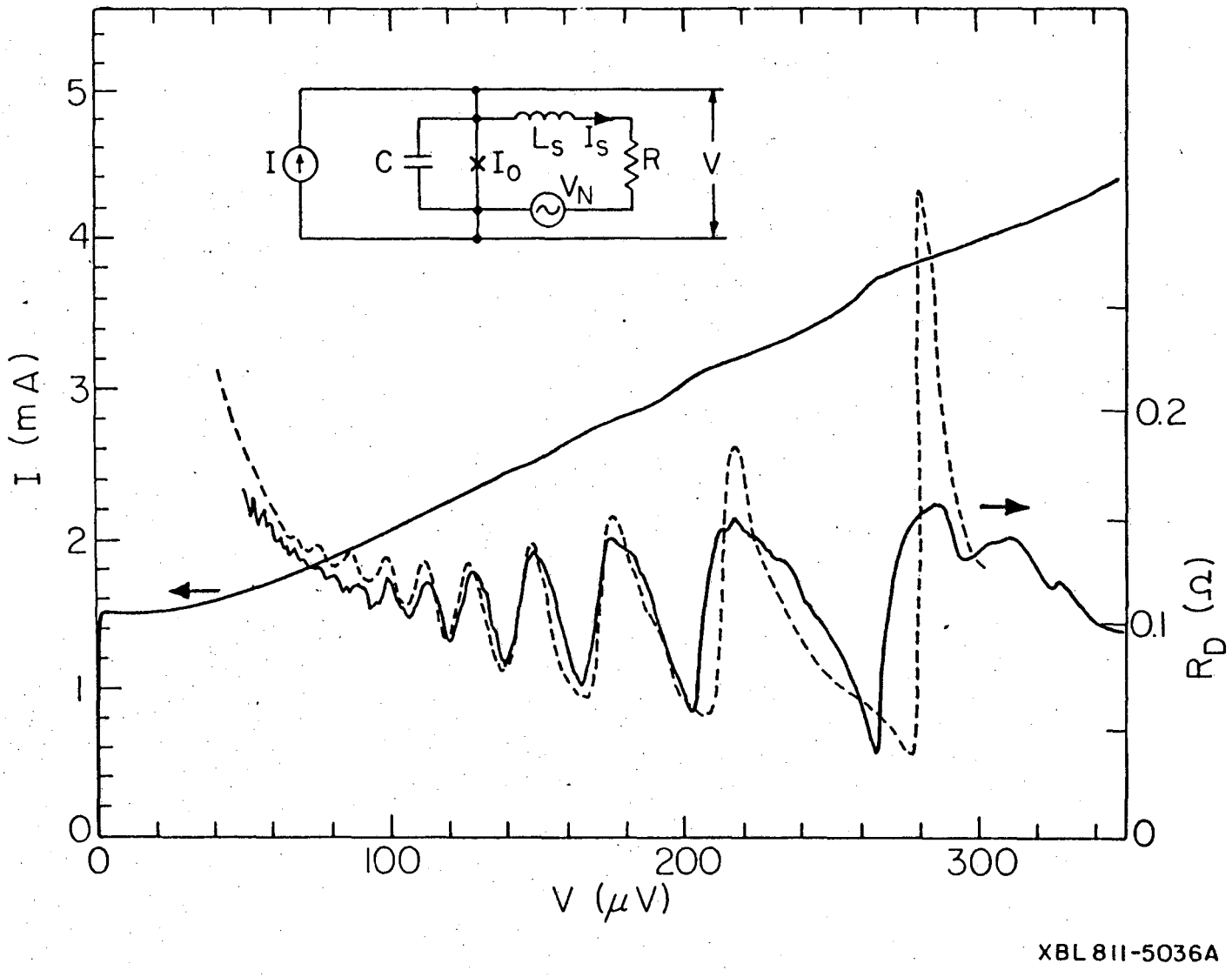
I
C
I_0
L_s
I_s
R
V
V_N
I (mA)
V (μV)
R_D (Ω)
0
1
2
3
4
5
0
100
200
300
0.1
0.2
XBL 811-5036A

Fig. 9

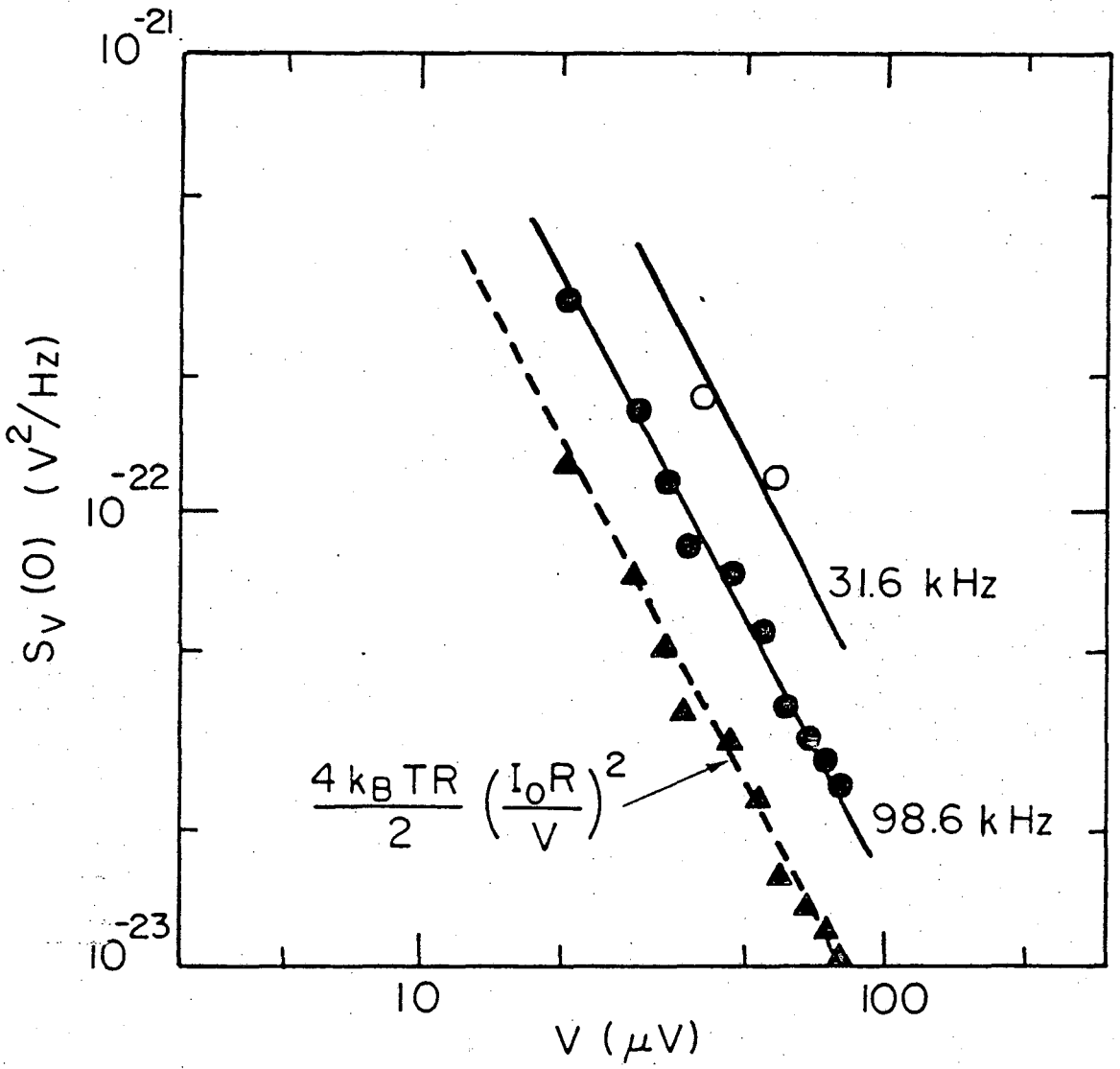

XBL 818-6314

Fig. 10

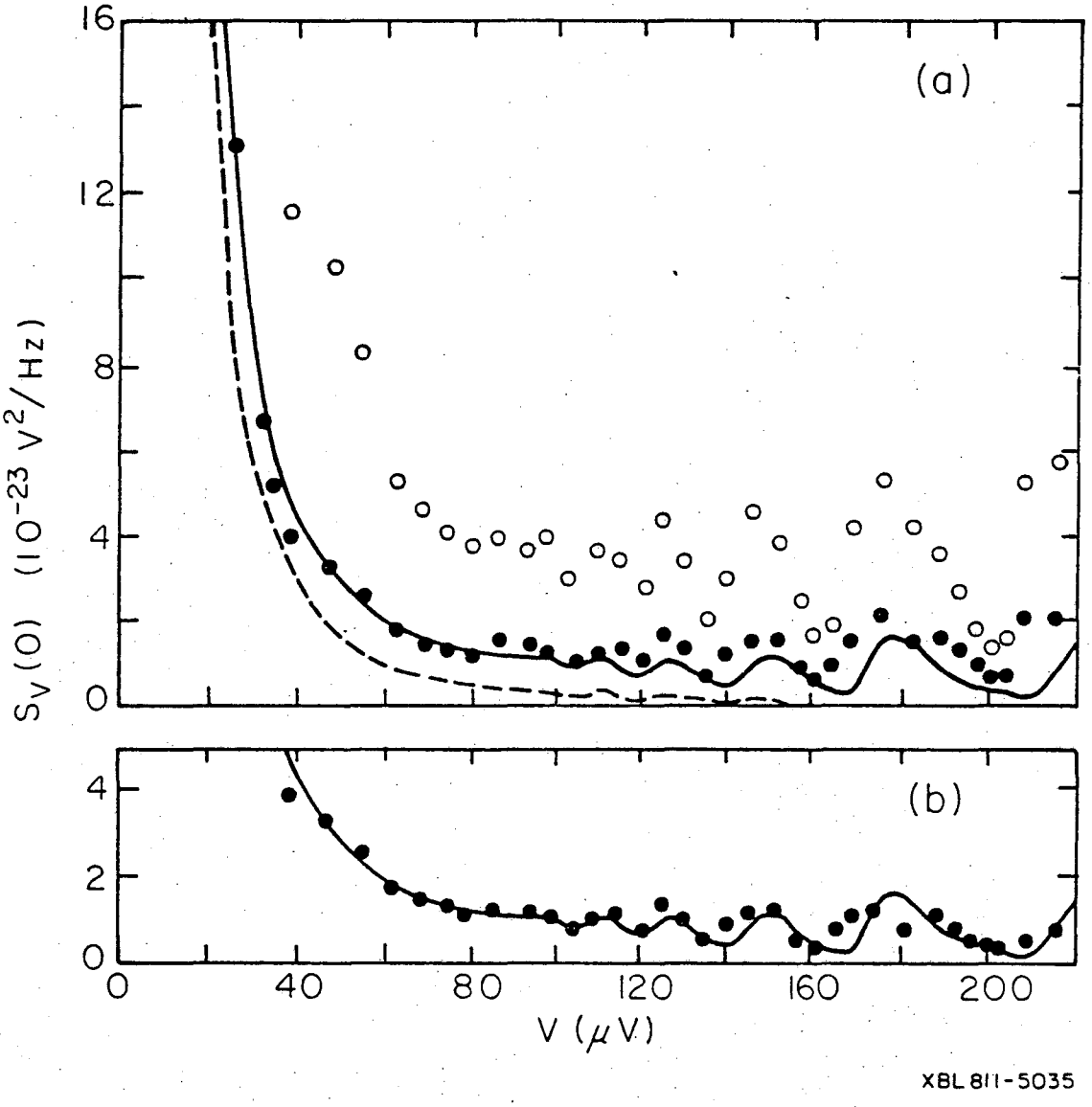
16
12
8
4
0
(a)
$S_V(0)$ $(10^{-23}\ V^2/Hz)$
4
2
0
(b)
0
40
80
120
160
200
V (μV)
XBL 811-5035

Fig. 11

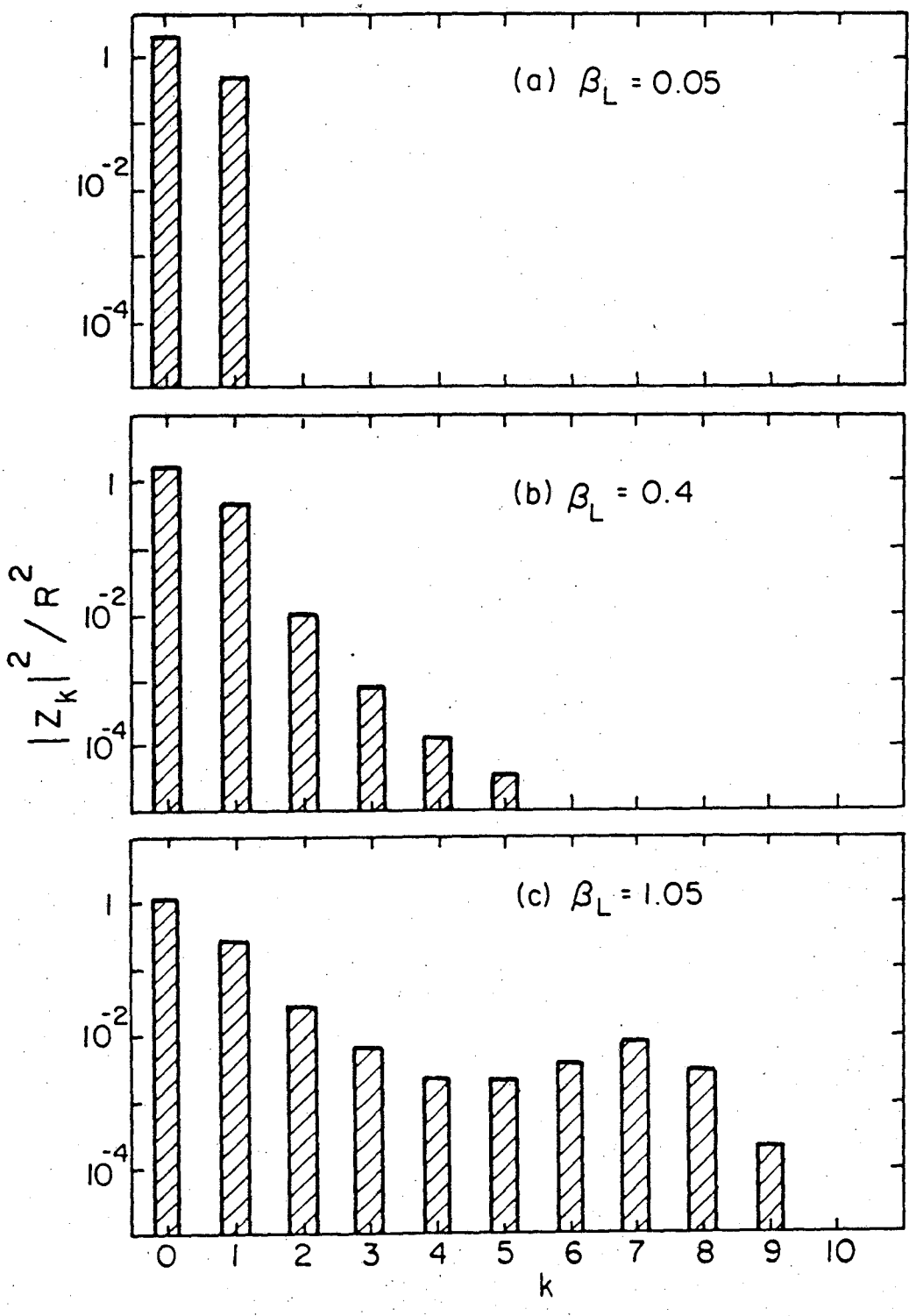
(a) $\beta_L = 0.05$
(b) $\beta_L = 0.4$
(c) $\beta_L = 1.05$
$|Z_k|^2/R^2$
1
10^{-2}
10^{-4}
0 1 2 3 4 5 6 7 8 9 10
k
XBL 818-6315

Fig. 12

This report was done with support from the Department of Energy. Any conclusions or opinions expressed in this report represent solely those of the author(s) and not necessarily those of The Regents of the University of California, the Lawrence Berkeley Laboratory or the Department of Energy.

Reference to a company or product name does not imply approval or recommendation of the product by the University of California or the U.S. Department of Energy to the exclusion of others that may be suitable.

TECHNICAL INFORMATION DEPARTMENT
LAWRENCE BERKELEY LABORATORY
UNIVERSITY OF CALIFORNIA
BERKELEY, CALIFORNIA 94720